Supporting information

Perfluoroalkyl Chain Length Effect on Crystal Packing and [LnO8] Coordination Geometry in Lanthanide-Lithium β- Diketonates: Luminescence and Single-Ion Magnet Behavior

Kristina A. Smirnova[1], Yulia O. Edilova[2], Mikhail A. Kiskin[3], Artem S. Bogomyakov[1], Yulia S. Kudyakova[2]*, Marina S. Valova[2], Galina V. Romanenko[1], Pavel A. Slepukhin[2], Victor I. Saloutin[2] and Denis N. Bazhin[2,4]*

[1] International Tomography Center, Siberian Branch of the Russian Academy of Sciences, 630090 Novosibirsk, Russian Federation
[2] Postovsky Institute of Organic Synthesis, Ural Branch of the Russian Academy of Sciences, 620137 Yekaterinburg, Russian Federation
[3] N.S. Kurnakov Institute of General and Inorganic Chemistry, Russian Academy of Sciences, 119991 Moscow, Russia
[4] Ural Federal University named after the First President of Russia B.N. Eltsin, Mira Str. 19, 620002, Ekaterinburg, Russian Federation
* Correspondence: yu.kudyakova@gmail.com, dnbazhin@gmail.com

Table S1. Crystallographic parameters and structure refinement statistics for **5**-**8**.

Code	**5** (R^F = C_2F_5)	**6** (R^F = C_2F_5)	**8** (R^F = C_2F_5)
Compound	[LiEu(L^2)$_4$(MeOH)]	[LiGd(L^2)$_4$(MeOH)]	[LiDy(L^2)$_4$(MeOH)]
Formula	$C_{37}H_{44}EuF_{20}LiO_{17}$	$C_{37}H_{44}F_{20}GdLiO_{17}$	$C_{37}H_{44}DyF_{20}LiO_{17}$
T (K)	250	250	296
FW	1298.61	1304.91	1310.16
Space group	P-1	P-1	P-1
Z	2	2	2
a, Å	11.1129(4)	11.1199(7)	11.1190(3)
b, Å	11.3025(5)	11.3337(7)	11.3357(3)
c, Å	23.0437(8)	23.0251(13)	22.9094(6)
α, °	76.651(1)	76.524(2)	76.297(1)
β, °	77.617(1)	77.560(2)	77.360(1)
γ, °	71.897(1)	71.625(2)	71.388(1)
V, Å^3	2644.71(18)	2646.2(3)	2626.27(12)
d_{calc}, g·cm^{-3}	1.631	1.638	1.657
θ_{min}-θ_{max} (deg)	1.926-39.381	2.28-32.12	4.021-67.679
μ(MoKα), mm^{-1}	1.319	1.386	8.848
h,k,l	-17 ≤ h ≤ 15 -17 ≤ k ≤ 16 -35 ≤ l ≤ 31	-15 ≤ h ≤ 15 -16 ≤ k ≤ 15 -32 ≤ l ≤ 32	-13 ≤ h ≤ 13 -13 ≤ k ≤ 13 -27 ≤ l ≤ 27
Number of reflections	32552	32956	42708
Unique reflections	18047	16007	9407
Reflections with I > 2σ(I)	11945	11609	8914
R_{int}	0.0314	0.0399	0.0306
F(000)	1294	1298	1302
Goof	1.030	1.034	1.037
R1 / wR2 for I > 2σI	0.0744 / 0.2064	0.0759 / 0.2049	0.0402 / 0.1084
R1 / wR2 for all data	0.1180 / 0.2389	0.1034 / 0.2349	0.0422 / 0.1103
CCDC	2258787	2258788	2255120

Table S1 (continued). Crystallographic parameters and structure refinement statistics for **9**-**11**. 17

Code	**9** (R^F = C_3F_7)	**10** (R^F = C_3F_7)	**11** (R^F = C_3F_7)
Compound	[LiEu(L^3)$_4$(MeOH)]	[LiGd(L^3)$_4$(MeOH)]	[LiTb(L^3)$_4$(MeOH)]
Formula	$C_{41}H_{44}EuF_{28}LiO_{17}$	$C_{41}H_{44}F_{28}GdLiO_{17}$	$C_{41}H_{44}TbF_{28}LiO_{17}$
T (K)	100(2)	100(2)	100
FW	1499.66	1504.95	1506.62
Space group	P-1	P-1	P-1
Z	2	2	2
a, Å	10.5787(19)	10.609(5)	10.5527(4)
b, Å	12.147(3)	12.079(4)	12.1312(5)
c, Å	22.571(5)	22.527(6)	22.4916(8)
α, °	98.146(14)	99.318(9)	98.494(1)
β, °	98.089(9)	98.930(12)	98.377(1)
γ, °	94.347(7)	94.48(2)	94.520(1)
V, Å^3	2829.0(10)	2798.3(18)	2802.49(19)
d_{calc}, g·cm^{-3}	1.761	1.786	1.785
θ_{min}-θ_{max} (deg)	2.48-30.61	2.30-31.13	2.31-30.42
μ(MoKα), mm^{-1}	1.265	1.343	1.420
h,k,l	-15 ≤ h ≤ 15	-16 ≤ h ≤ 15	-14 ≤ h ≤ 13
	-16 ≤ k ≤ 17	-14 ≤ k ≤ 18	-16 ≤ k ≤ 16
	-32 ≤ l ≤ 32	-34 ≤ l ≤ 34	-30 ≤ l ≤ 30
Number of reflections	31270	33910	27394
Unique reflections	16954	18970	14368
Reflections with I > 2σ(I)	15536	15394	12791
R_{int}	0.0219	0.0315	0.0245
F(000)	1488	1490	1492
Goof	1.063	1.082	1.049
R1 / wR2 for I > 2σI	0.0376 / 0.0978	0.0572 / 0.1222	0.0431 / 0.1075
R1 / wR2 for all data	0.0423 / 0.0978	0.0790 / 0.1325	0.0501 / 0.1114
CCDC	2258789	2258790	2258791

18

Table S1 (continued). Crystallographic parameters and structure refinement statistics for **12**-**14**. 19

Code	**12** (R^F = C_4F_9)	**13** (R^F = C_4F_9)	**14** (R^F = C_4F_9)
Compound	[LiEu(L^4)$_4$(MeOH)]	[LiGd(L^4)$_4$(MeOH)]	[LiTb(L^4)$_4$(MeOH)]
Formula	$C_{45}H_{44}EuF_{36}LiO_{17}$	$C_{45}H_{44}F_{36}GdLiO_{17}$	$C_{45}H_{44}TbF_{36}LiO_{17}$
T (K)	100(2)	100.0	100.0
FW	1699.70	1704.99	1706.66
Space group	P-1	P-1	P-1
Z	2	2	2
a, Å	10.4566(4)	10.4696(13)	10.6905(6)
b, Å	13.7470(5)	13.756(2)	14.5385(8)
c, Å	22.4166(8)	22.417(3)	22.0395(12)
α, °	98.2860(10)	98.181(5)	102.861(2)
β, °	100.4410(10)	100.306(5)	98.191(2)
γ, °	90.4630(10)	90.527(6)	105.287(2)
V, Å^3	3133.9(2)	3142.1(8)	3146.8(3)
d_{calc}, g·cm^{-3}	1.801	1.802	1.801
θ_{min}-θ_{max} (deg)	2.34-33.08	2.46-32.94	2.422-30.57
μ(MoKα), mm^{-1}	1.171	1.226	1.294

h,k,l	-15 ≤ h ≤ 15	-15 ≤ h ≤ 15	-12 ≤ h ≤ 14
	-21 ≤ k ≤ 19	-18 ≤ k ≤ 20	-19 ≤ k ≤ 19
	-32 ≤ l ≤ 34	-34 ≤ l ≤ 33	-29 ≤ l ≤ 29
Number of reflections	37710	38285	28413
Unique reflections	21295	21278	15503
Reflections with I > 2σ(I)	17976	18791	14046
R_{int}	0.0256	0.0225	0.0207
$F(000)$	1680	1682	1684
Goof	1.049	1.050	1.052
R1 / wR2 for I > 2σI	0.0534 / 0.1347	0.0453 / 0.1131	0.0368 / 0.0936
R1 / wR2 for all data	0.0670 / 0.1429	0.0536 / 0.1184	0.0421 / 0.0936
CCDC	2258792	2258793	2258794

Table S1 (continued). Crystallographic parameters and structure refinement statistics for **15**.

Code	**15** ($R^F = C_4F_9$)
Compound	$[LiDy(L^4)_4(MeOH)]$
Formula	$C_{45}H_{44}DyF_{36}LiO_{17}$
T (K)	240
FW	1710.24
Space group	P-1
Z	2
a, Å	11.0001(4)
b, Å	14.8467(5)
c, Å	22.0163(7)
α, °	102.473(2)
β, °	98.063(2)
γ, °	106.5187(17)
V, Å^3	3286.8(2)
d_{calc}, g·cm^{-3}	1.728
θ_{min}-θ_{max} (deg)	3.22-66.83
μ(MoKα), mm^{-1}	7.599
h,k,l	-13 ≤ h ≤ 12
	-17 ≤ k ≤ 17
	-26 ≤ l ≤ 26
Number of reflections	42583
Unique reflections	11760
Reflections with I > 2σ(I)	10270
R_{int}	0.1380
$F(000)$	1686
Goof	1.055
R1 / wR2 for I > 2σI	0.0821 / 0.2076
R1 / wR2 for all data	0.0879 / 0.2144
CCDC	2255119

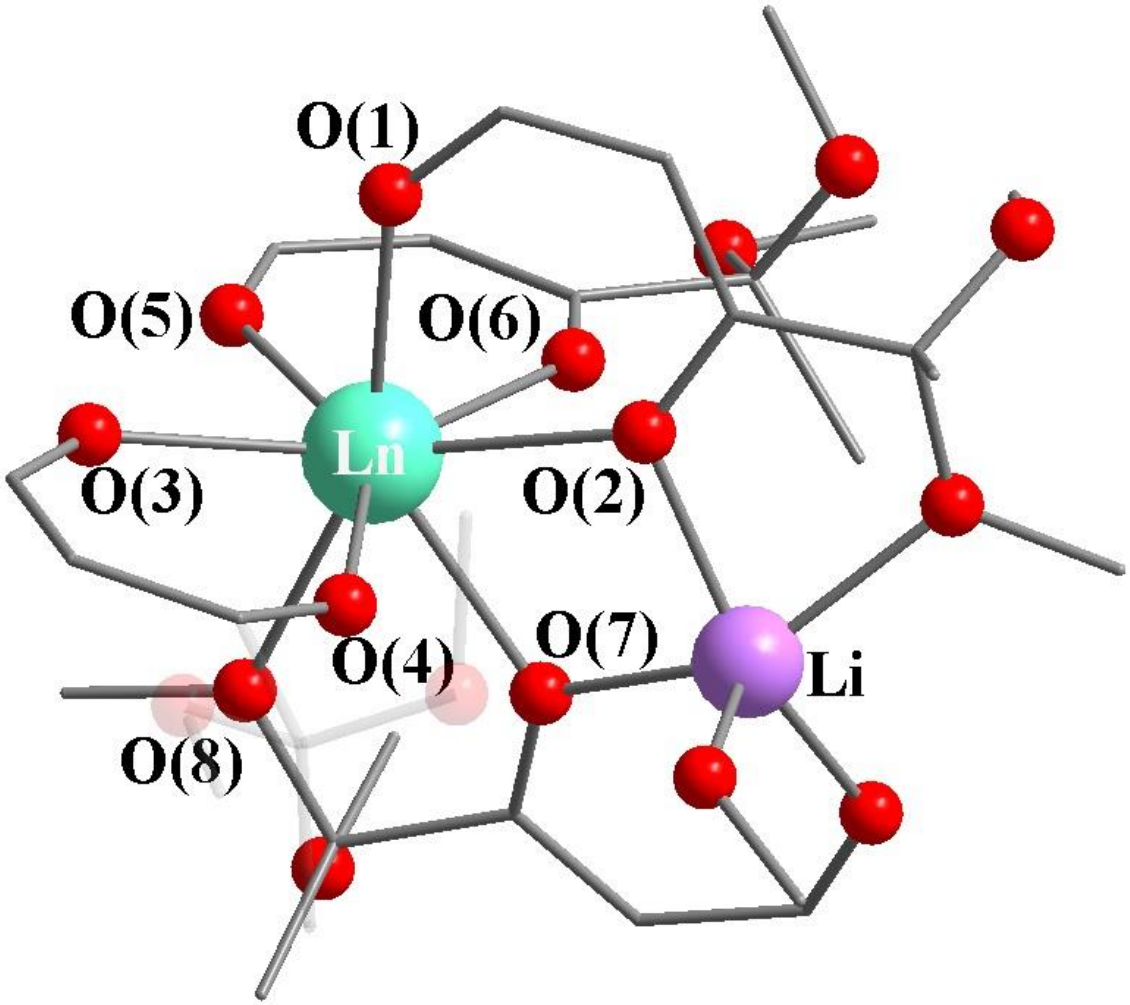

Figure S1 The structures of heterometallic framework of complexes **1**-**15**

Table S2. Selected angles (°) in [Eu-Li] β-diketonates **1**, **5**, **9**, **12**.

	Eu *tris*-diketonate fragment		
	∠ O(1)-Eu-O(2)	∠ O(3)-Eu-O(4)	∠ O(5)-Eu-O(6)
1	70.66(14)	71.32(15)	70.33(17)
5	70.72(17)	71.39(16)	70.83(17)
9	74.58(36)/69.27(19)	71.39(6)	70.69(7)
12	71.68(8)	71.48(7)	70.99(8)
	Eu-Li heterometallic fragment		
	∠ O(2)-Eu-O(7)	∠ Eu-O(2)-Li	∠ Eu-O(7)-Li
1	67.99(13)	103.667(323)	104.72(35)
5	67.55(15)	103.22(41)	105.98(39)
9	66.53(7)	104.59(17)	106.04(16)
12	68.49(8)	103.72(18)	104.69(18)
	LiL coordination with EuL_3		
	1	**5**	**9**	**12**
∠ O(7)-Dy-O(8)	61.83(12)	62.57(14)	61.88(6)	63.303(7)

Table S3. Selected angles (°) in [Gd-Li] β-diketonates **2**, **6**, **10**, **13**.

	Gd *tris*-diketonate fragment		
	∠ O(1)-Gd-O(2)	∠ O(3)-Gd-O(4)	∠ O(5)-Gd-O(6)
2	71.05(16)°	71.58(16)°	70.89(19)°
6	70.72(17)°	71.394(16)°	70.83(17)°
10	71.29(11)	71.80(9)°	71.14(11)°
13	71.13(7)°	71.25(7)°	70.76(8)°
	Gd-Li heterometallic fragment		
	∠ O(2)-Gd-O(7)	∠ Gd-O(2)-Li	∠ Gd-O(7)-Li
2	68.18(16)°	103.44(38)°	104.55(40)°
6	67.55(15)°	103.22(41)°	105.98(39)°
10	66.73(10)°	104.34(24)°	106.48(25)°
13	67.54(7)°	103.63(17)°	105.49(18)°
	LiL coordination with GdL_3		
	2	**6**	**10**	**13**
∠ O(7)-Gd-O(8)	61.99(15)°	62.57(14)°	62.86(10)°	62.44(8)°

Table S4. Selected angles (°) in [Tb-Li] β-diketonates **3**, **7**, **11**, **14**.

	Tb *tris*-diketonate fragment		
	∠ O(1)-Tb-O(2)	∠ O(3)-Tb-O(4)	∠ O(5)-Tb-O(6)
3	71.45(14)°	71.904(144)°	71.240(174)°
7	71.22(17)°	71.747(165)°	71.077(156)°
11	74.88(35)°/68.93 (28)°	71.908(77)°	71.100(96)°
14	70.84(8)°	71.029(78)°	70.522(89)°
	Tb-Li heterometallic fragment		
	∠ O(2)-Tb-O(7)	∠ Tb-O(2)-Li	∠ Tb-O(7)-Li
3	68.38(14)°	102.67(36)°	104.21(38)°
7	68.37(15)°	103.27(40)°	105.91(39)°
11	66.81(8)°	104.70(22)°	106.63(23)°
14	67.51(8)°	103.60(21)°	105.37(22)°
	LiL coordination with TbL_3		
	3	**7**	**11**	**14**
∠ O(7)-Tb-O(8)	62.45(14)°	62.85(15)°	62.50(8)°	62.23(9)°

Table S5. Selected angles (°) in [Dy-Li] β-diketonates **4**,**8**,**15**,**16**.

	Dy *tris*-diketonate fragment		
	∠ O(1)-Dy-O(2)	∠ O(3)-Dy-O(4)	∠ O(5)-Dy-O(6)
4	71.75(15)°	72.22(16)°	71.27(19)°
8	71.45(10)°	72.11(11)°	71.57(10)°
15	71.62(16)°	71.63(15)°	71.37(17)°
16	71.58(8)°	72.48(8)°	70.77(8)°
	Dy-Li heterometallic fragment		
	∠ O(2)-Dy-O(7)	∠ Dy-O(2)-Li	∠ Dy-O(7)-Li
4	68.42(15)°	103.00(37)°	104.60(43)°
8	68.18(8)°	103.76(24)°	106.11(23)°
15	69.09(15)°	103.24(39)°	104.93(38)°
16	67.52(7)°	104.35(18)°	106.29(18)°
	LiL coordination with DyL_3		
	4	**8**	**15**	**16**
∠ O(8)-Dy-O(7)	62.69(15)°	63.37(9)°	63.43(15)°	63.40(7)°

Table S6. Selected bond distances in [Eu-Li] β-diketonates **1**, **5**, **9**, **12**.

Parameter, Å	**1** ($R^F = CF_3$)	**5** ($R^F = C_2F_5$)	**9** ($R^F = C_3F_7$)	**12** ($R^F = C_4F_9$)
Li–O	1.93(1)–2.02(1)	1.9095(139)–2.0993(163)	1.928(46)-2.015(5)	1.917(7)–2.030(8)
Eu–O	2.335(5)–2.399(5)	2.3332(59)–2.3635(44)	2.287(14)–2.380(2)/ 2.262(2)-2.393(8)	2.329(2)–2.402(3)
Eu–O(2)	2.426(3)	2.429(4)	2.440(2)	2.432(3)
Eu–O(8)	2.534(4)	2.501(5)	2.521(2)	2.517(3)
Li...Eu	3.498(11)	3.500(11)	3.534(5)	3.491(7)
Eu…Eu	10.5273(5)	11.1129(5)	10.579(2)	10.457(5)
	11.2632(5)	11.3025(6)	11.088(2)	10.8817(7)
	12.1561(7)	11.6611(7)	12.147(3)	12.3805(7)
	12.2251(5)	12.0714(7)	12.606(3)	13.7470(6)
	12.4277(5)	13.4775(6)	12.655(3)	
	13.0570(5)			

Table S7. Selected bond distances in [Gd-Li] β-diketonates **2**, **6**, **10**, **13**.

Parameter, Å	**2** ($R^F = CF_3$)	**6** ($R^F = C_2F_5$)	**10** ($R^F = C_3F_7$)	**13** ($R^F = C_4F_9$)
Li–O	1.940(15)–2.033(13)	1.931(13)–2.086(15)	1.922(7)–2.034(8)	1.913(5)–2.025(6)
Gd–O	2.322(6)–2.380(6)	2.315(6)–2.364(5)	2.331(4)–2.394(3)	2.322(2)–2.397(2)
Gd–O(2)	2.411(5)	2.417(4)	2.428(3)	2.424(2)
Gd–O(8)	2.529(5)	2.496(5)	2.501(3)	2.506(2)
Li...Gd	3.479(12)	3.491(11)	3.514(7)	3.484(6)
Gd…Gd	10.5643(6)	11.1199(8)	10.609(5)	10.470(1)
	11.2950(6)	11.3337(9)	11.005(3)	10.902(2)
	12.2645(7)	11.6509(8)	12.079(4)	12.360(2)
	12.4283(6)	12.04228(8)	12.539(3)	12.400(2)
	13.0551(6)	14.0594(9)	12.596(3)	14.277(2)

Table S8. Selected bond distances in [Tb-Li] β-diketonates **3**,**7**,**11**,**14**.

Parameter, Å	**3** ($R^F = CF_3$)	**7** ($R^F = C_2F_5$)	**11** ($R^F = C_3F_7$)	**14** ($R^F = C_4F_9$)
Li–O	1.930(15)–2.042(12)	1.939(14)–2.069(15)	1.913(7)–2.030(8)	1.922(4)–2.050(6)
Tb–O	2.301(4)–2.371(6)	2.291(6)–2.356(4)	2.251(13)–2.375(3)/ 2.332(2)-2.380(11)	2.316(2)–2.365(2)
Tb–O(2)	2.4040(32)	2.4079(39)	2.407(2)	2.394(2)
Tb–O(8)	2.5057(36)	2.4933(54)	2.484(2)	2.460(2)
Li...Tb	3.4711(118)	3.4856(106)	3.515(7)	3.469(5)
Tb…Tb	10.5516(5)	11.1199(6)	10.5527(5)	10.6905(7)
	11.2525(6)	11.5161(7)	11.0231(7)	11.1753(8)
	12.1678(7)	11.5588(6)	12.1312(6)	12.3621(9)
	12.1989(4)	11.9528(6)	12.5623(7)	12.3621(8)
	12.3967(5)	13.4494(7)		14.5385(9)
	12.9985(5)			

Table S9. Selected bond distances in [Dy-Li] β-diketonates **4**,**8**,**15**,**16**.

Parameter	**4** ($R^F = CF_3$)	**8** ($R^F = C_2F_5$)	**15** ($R^F = C_4F_9$)	**16** ($R^F = CF_3$)
Li–O	1.939(17)–2.041(13)	1.925(9)–2.030(9)	1.924(10)–2.054(14)	1.924(7)–2.047(6)
Dy–O	2.297(6)–2.357(6)	2.220(4)–2.330(3)	2.298(4)–2.355(5)	2.311(2)–2.363(2)
Dy–O(2)	2.395(3)	2.390(2)	2.392(5)	2.383(2)
Dy–O(8)	2.506(5)	2.465(3)	2.464(5)	2.496(2)
Li...Dy	3.452(13)	3.485(7)	3.462(10)	3.462(5)
Dy…Dy	10.6105(5)	11.1190(5)	11.0001(6)	9.6333(3)
	11.3166(5)	11.3357(5)	11.1695(7)	11.2038(3)
	12.2197(5)	11.5825(6)	12.1864(7)	11.3081(3)
	12.3203(5)	11.9606(6)	14.8467(7)	11.9719(3)
	12.4237(5)	13.1025(4)		12.2177(3)
	13.0283(5)	13.4274(6)		12.4342(3)

Table S10. Continuous shape measures (CShM) calculations values for **Eu-Li** complexes using SHAPE.

	1 ($R^F = CF_3$)	**5** ($R^F = C_2F_5$)	**9** ($R^F = C_3F_7$)	**12** ($R^F = C_4F_9$)
Octagon (OP-8), D_{8h}	32.224	32.856	34.587/32.323	33.967
Heptagonal pyramid (HPY-8), C_{7v}	23.884	24.163	22.148/22.232	23.251
Hexagonal bipyramid (HBPY-8), D_{6h}	15.728	16.147	13.389/14.363	14.676
Cube (CU-8), O_h	11.618	11.967	10.677/10.505	11.695
Square antiprism (SAPR-8), D_{4d}	2.160	2.847	3.798/2.649	3.338
Triangular dodecahedron (TDD-8), D_{2d}	1.315	1.055	2.707/2.473	2.015
Johnson gyrobifastigium J26 (JGBF-8), D_{2d}	12.782	12.498	11.429/12.226	12.265
Johnson elongated triangular bipyramid J14 (JETBPY-8), D_{3h}	29.730	28.943	26.849/26.889	27.553
Biaugmented trigonal prism J50 (JBTPR-8), C_{2v}	2.523	2.665	2.825/2.486	2.673
Biaugmented trigonal prism (BTPR-8), C_{2v}	1.983	2.123	2.052/1.877	1.932
Snub diphenoid J84 (JSD-8), D_{2d}	3.755	3.293	4.958/4.538	4.285
Triakis tetrahedron (TT-8), T_d	12.252	12.748	11.275/11.048	12.312
Elongated trigonal bipyramid (ETBPY-8), D_{3h}	24.267	25.082	22.949/21.895	23.725

Table S11. Continuous shape measures (CShM) calculations values for **Gd-Li** complexes using SHAPE.

	2 ($R^F = CF_3$)	**6** ($R^F = C_2F_5$)	**10** ($R^F = C_3F_7$)	**13** ($R^F = C_4F_9$)
Octagon (OP-8), D_{8h}	31.854	32.825	33.555	33.771
Heptagonal pyramid (HPY-8), C_{7v}	23.920	24.222	22.833	23.310
Hexagonal bipyramid (HBPY-8), D_{6h}	15.908	16.144	14.092	14.678
Cube (CU-8), O_h	11.652	11.873	10.596	11.657
Square antiprism (SAPR-8), D_{4d}	2.015	2.813	2.978	3.235
Triangular dodecahedron (TDD-8), D_{2d}	1.253	1.003	2.370	1.963
Johnson gyrobifastigium J26 (JGBF-8), D_{2d}	12.969	12.575	12.158	12.307
Johnson elongated triangular bipyramid J14 (JETBPY-8), D_{3h}	29.866	29.062	27.290	27.618
Biaugmented trigonal prism J50 (JBTPR-8), C_{2v}	2.487	2.662	2.435	2.611
Biaugmented trigonal prism (BTPR-8), C_{2v}	1.941	2.101	1.728	1.868
Snub diphenoid J84 (JSD-8), D_{2d}	3.691	3.279	4.625	4.231
Triakis tetrahedron (TT-8), T_d	12.311	12.674	11.179	12.279
Elongated trigonal bipyramid (ETBPY-8), D_{3h}	24.342	25.143	23.780	23.849

Table S12. Continuous shape measures (CShM) calculations values for **Tb-Li** complexes using SHAPE.

	3 ($R^F = CF_3$)	**7** ($R^F = C_2F_5$)	**11** ($R^F = C_3F_7$)	**14** ($R^F = C_4F_9$)
Octagon (OP-8), D_{8h}	31.870	32.867	34.187/32.279	31.650
Heptagonal pyramid (HPY-8), C_{7v}	24.096	24.279	22.277/22.527	23.701
Hexagonal bipyramid (HBPY-8), D_{6h}	15.930	16.122	13.534/14.577	16.691
Cube (CU-8), O_h	11.669	11.724	10.753/10.634	11.734
Square antiprism (SAPR-8), D_{4d}	2.036	2.752	3.652/2.463	3.152
Triangular dodecahedron (TDD-8), D_{2d}	1.134	0.986	2.681/2.292	0.947
Johnson gyrobifastigium J26 (JGBF-8), D_{2d}	12.971	12.703	11.680/12.493	13.080
Johnson elongated triangular bipyramid J14 (JETBPY-8), D_{3h}	29.919	29.116	27.137/27.229	28.611
Biaugmented trigonal prism J50 (JBTPR-8), C_{2v}	2.421	2.558	2.756/2.367	3.151
Biaugmented trigonal prism (BTPR-8), C_{2v}	1.902	2.012	1.966/1.764	2.487
Snub diphenoid J84 (JSD-8), D_{2d}	3.549	3.322	4.836/4.363	3.292
Triakis tetrahedron (TT-8), T_d	12.500	12.557	11.386/11.181	12.551
Elongated trigonal bipyramid (ETBPY-8), D_{3h}	24.569	25.263	23.213/22.207	24.838

Table S13. Continuous shape measures (CShM) calculations values for **Dy-Li** complexes using SHAPE.

	4 (R^F = CF_3)	**8** (R^F = C_2F_5)	**15** (R^F = C_4F_9)	**16** (R^F = CF_3)
Octagon (OP-8), D_{8h}	31.536	32.726	32.594	32.204
Heptagonal pyramid (HPY-8), C_{7v}	24.081	24.468	23.837	21.911
Hexagonal bipyramid (HBPY-8), D_{6h}	15.916	16.193	17.068	13.248
Cube (CU-8), O_h	11.638	11.680	11.349	10.089
Square antiprism (SAPR-8), D_{4d}	1.909	2.790	3.593	3.487
Triangular dodecahedron (TDD-8), D_{2d}	1.144	0.894	0.911	1.777
Johnson gyrobifastigium J26 (JGBF-8), D_{2d}	13.036	12.646	13.414	11.748
Johnson elongated triangular bipyramid J14 (JETBPY-8), D_{3h}	30.086	29.193	28.794	27.092
Biaugmented trigonal prism J50 (JBTPR-8), C_{2v}	2.386	2.597	2.943	2.851
Biaugmented trigonal prism (BTPR-8), C_{2v}	1.862	2.040	2.255	1.990
Snub diphenoid J84 (JSD-8), D_{2d}	3.592	3.149	3.407	4.053
Triakis tetrahedron (TT-8), T_d	12.407	12.497	12.127	10.654
Elongated trigonal bipyramid (ETBPY-8), D_{3h}	24.387	25.436	25.277	22.407

Table S14. Dihedral angles between the LnOO and β-diketonate (**L**) planes in the crystals of complexes.

Dihedral angle between planes (°)	R^F = CF_3 (**1**-**4**)	R^F = C_2F_5 (**5**-**8**)	R^F = C_3F_7 (**9**-**11**)	R^F = C_4F_9 (**12**-**15**)	R^F = CF_3 (**16**)
EuOO-**L**(1)	12	9	13/8	13	
EuOO-**L**(2)	3	7	23	28	
EuOO-**L**(3)	5	4	0.7	0.9	-
EuOO-**L**(bridging)	10	7	13	11	
sum of angles	30	27	50/45	53	
GdOO-**L**(1)	11	9	12	13	
GdOO-**L**(2)	3	7	23	28	
GdOO-**L**(3)	5	4	1	1	-
GdOO-**L**(bridging)	13	7	8	10	
sum of angles	32	27	44	52	
TbOO-**L**(1)	12	10	14/9	10	
TbOO-**L**(2)	4	9	22	24	
TbOO-**L**(3)	4	3	1	9	-
TbOO-**L**(bridging)	13	6	12	6	
sum of angles	33	28	49/44	49	
DyOO-**L**(1)	11	10		9	12
DyOO-**L**(2)	3	7		22	10
DyOO-**L**(3)	5	4	-	8	15
DyOO-**L**(bridging)	10	12		14	1
sum of angles	29	33		53	38

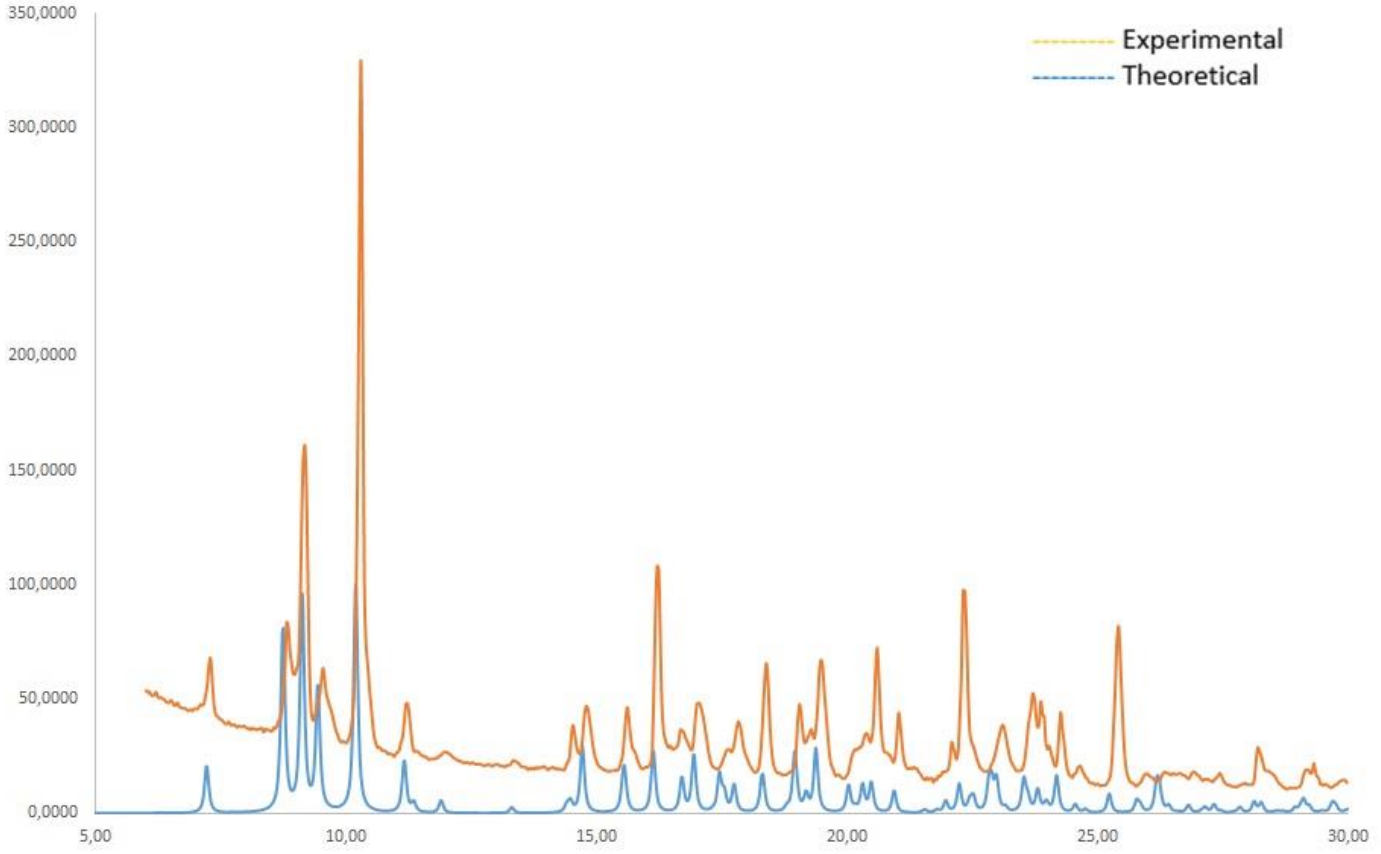

46

Figure S2 .PXRD for CF_3-β-diketonate **4** (yellow line – experimental, blue line – calculated (according to single crystal X-ray data)) 47

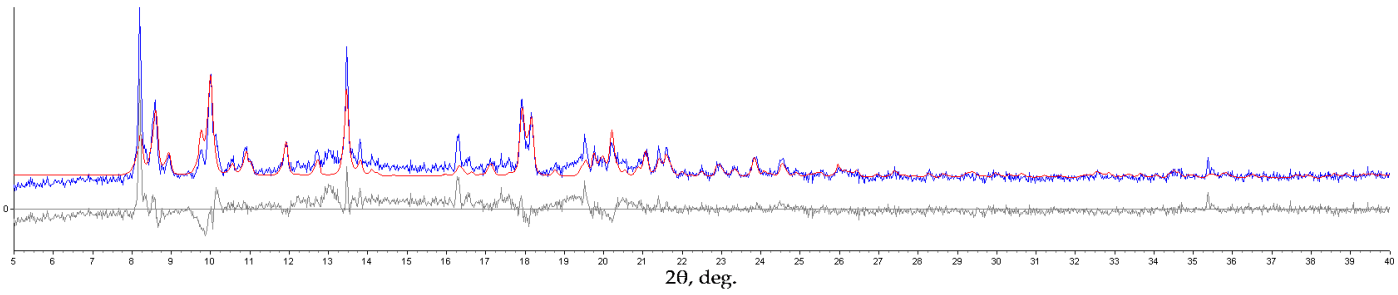

48

Figure S3 .PXRD for C_2F_5-β-diketonate **7** (blue line – experimental; red line – calculated (using the TOPAS software [TOPAS Software. Version 4.2. Karlsruhe: Bruker AXS, 2009])) 49 50

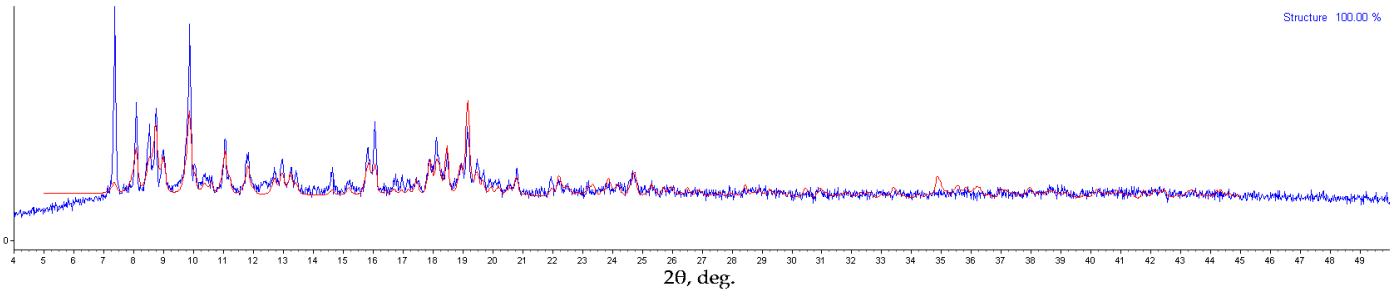

51

Figure S4 .PXRD for C_3F_7-β-diketonate **10** (blue line – experimental; red line – calculated (using the TOPAS software [TOPAS Software. Version 4.2. Karlsruhe: Bruker AXS, 2009])) 52 53

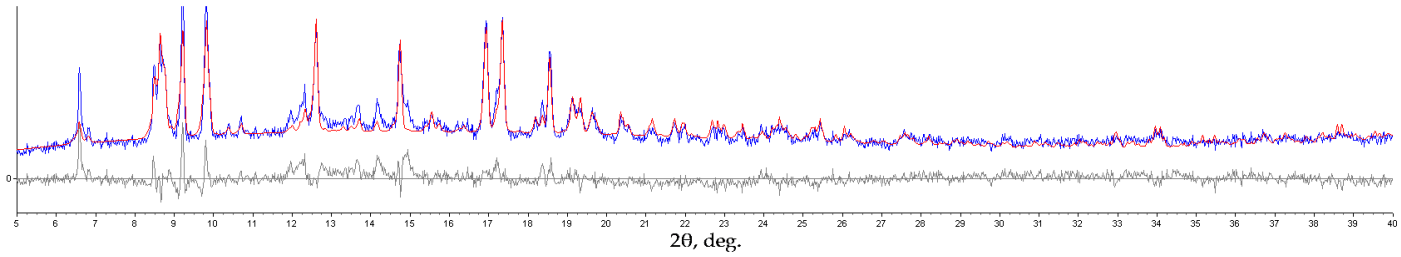

Figure S5 .PXRD for C_4F_9-β-diketonate **14** (blue line – experimental; red line – calculated (using the TOPAS software [TOPAS Software. Version 4.2. Karlsruhe: Bruker AXS, 2009]))

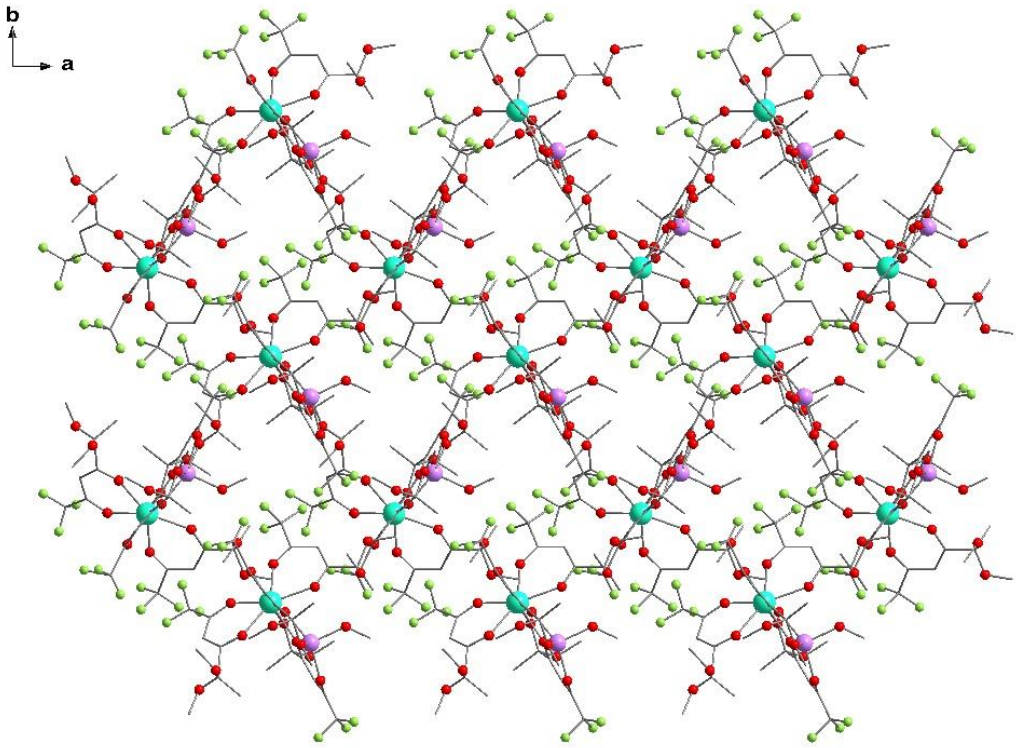

a

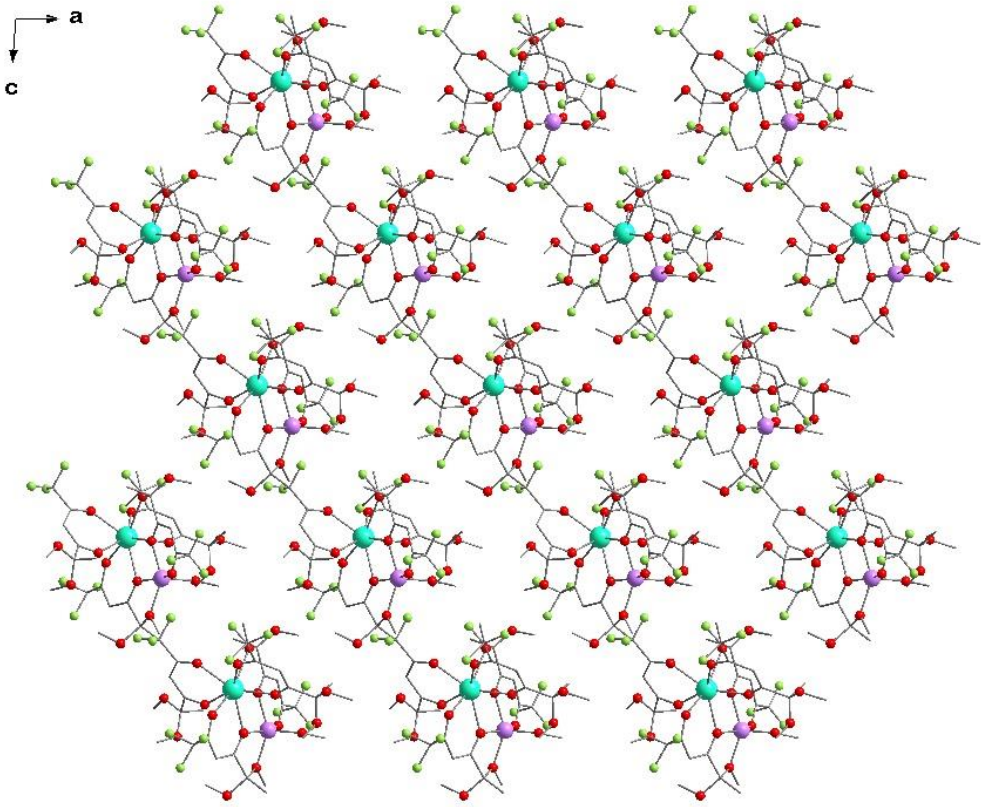

b

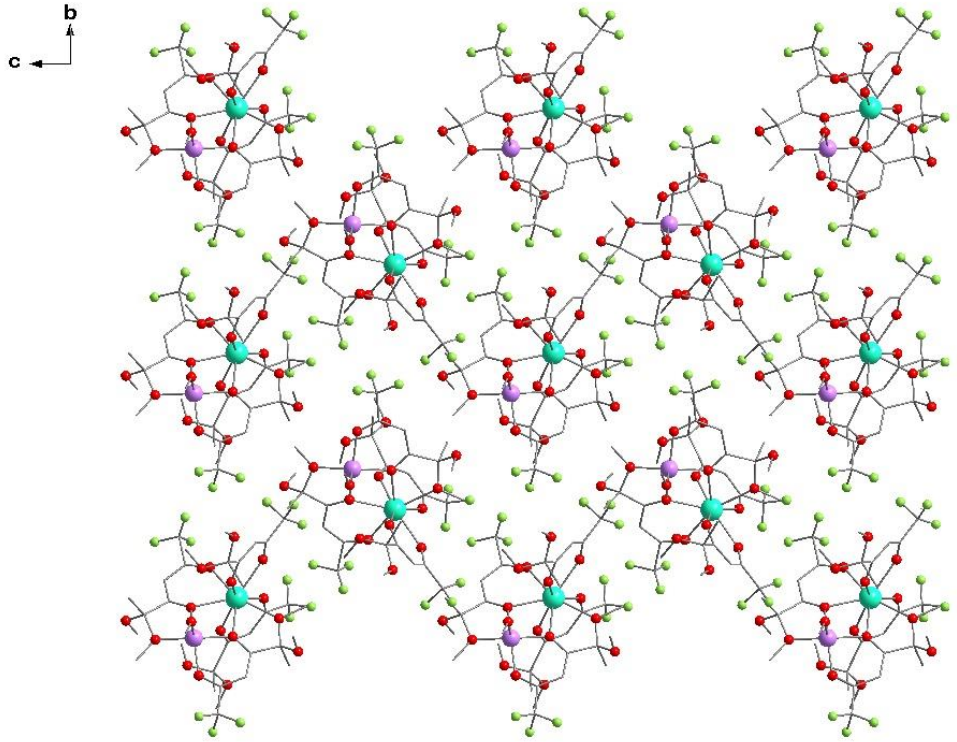

c

Figure S6. Crystal packing of trifluoromethylated Ln-Li β-diketonates **1**-**4** along *c* (**a**), *b* (**b**) and *a* (**c**) axis.

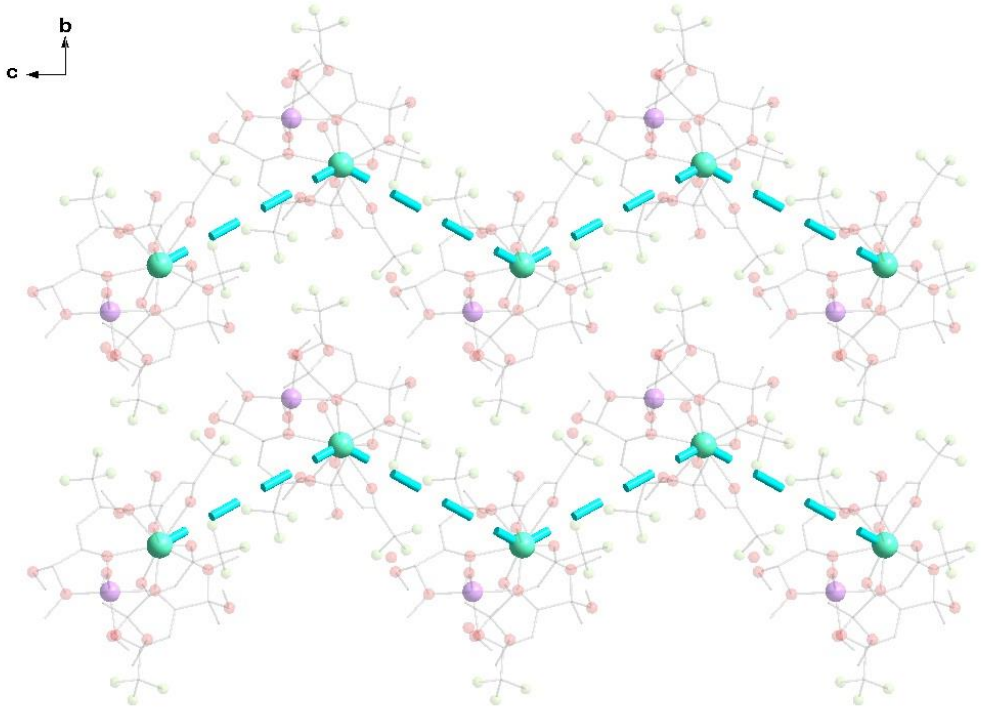

Figure S7. Two 1D chains of trifluoromethylated Ln-Li β-diketonates **1**-**4** with the shortest Ln…Ln distance (dashed line). Eu(1)…Eu(2) = 10.5273(5) Å, Gd(1)…Gd(2) = 10.5643(6) Å, Tb(1)…Tb(2) = 10.5516(5) Å, Dy(1)…Dy(2) = 10.6105(5) Å, ∠Eu(1)-Eu(2)-Eu(3) = 131.445(4)°, ∠Gd(1)-Gd(2)-Gd(3) = 131.411(4)°, ∠Tb(1)- Tb(2)- Tb(3) = 131.139(4)°, ∠Dy(1)-Dy(2)-Dy(3) = 130.966(4)°.

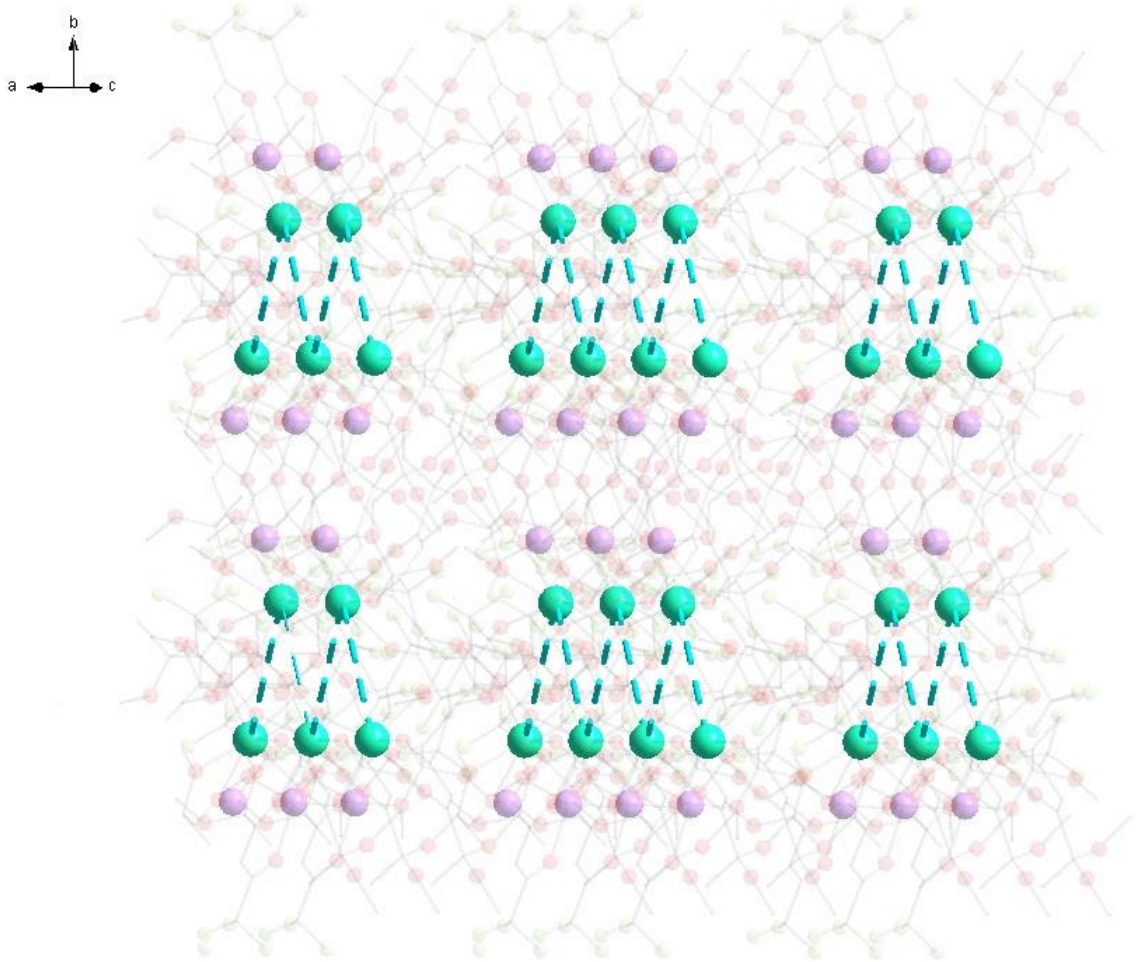

Figure S8. 1D chains packing of trifluoromethylated Ln-Li β-diketonates **1**-**4** with the shortest Ln…Ln distance (dashed line).

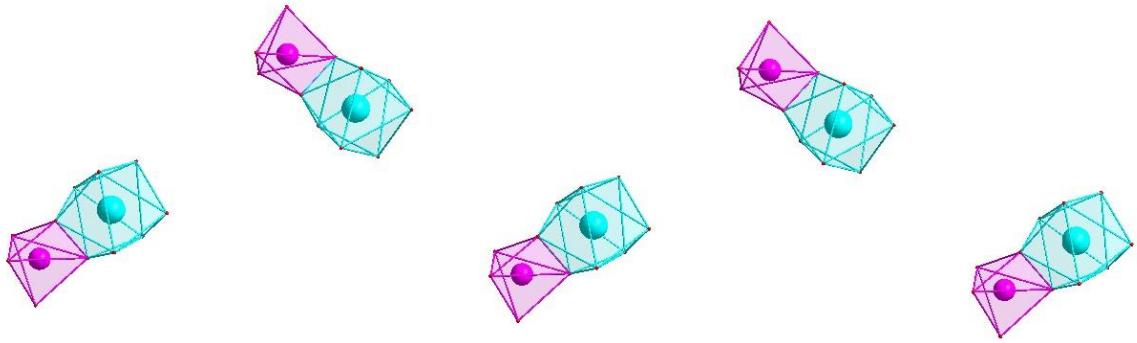

Figure S9. 1D chain of trifluoromethylated Ln-Li β-diketonates **1-4** (polyhedral [LnO_8] and [LiO_5] views only) with the shortest Ln…Ln distance.

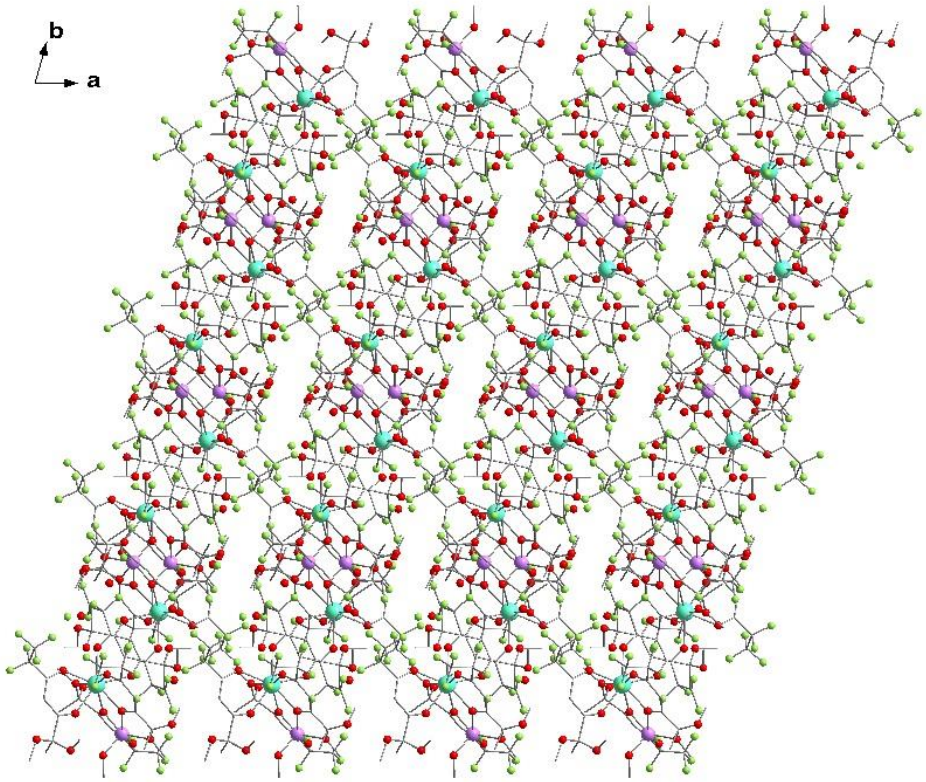

77

a

78

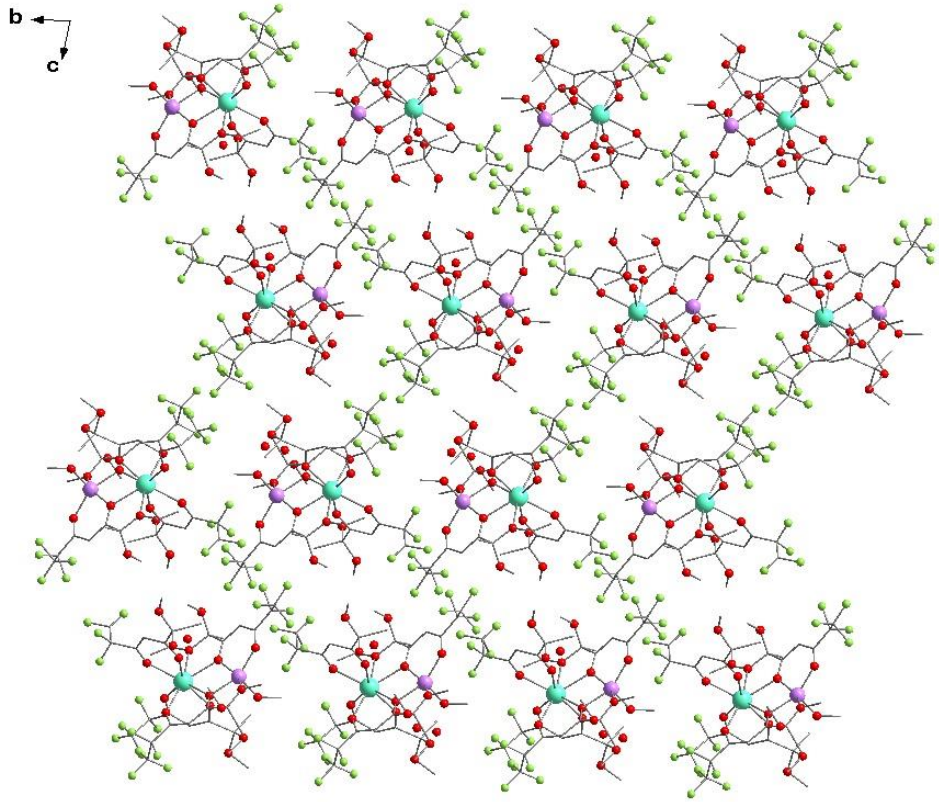

79

b

80

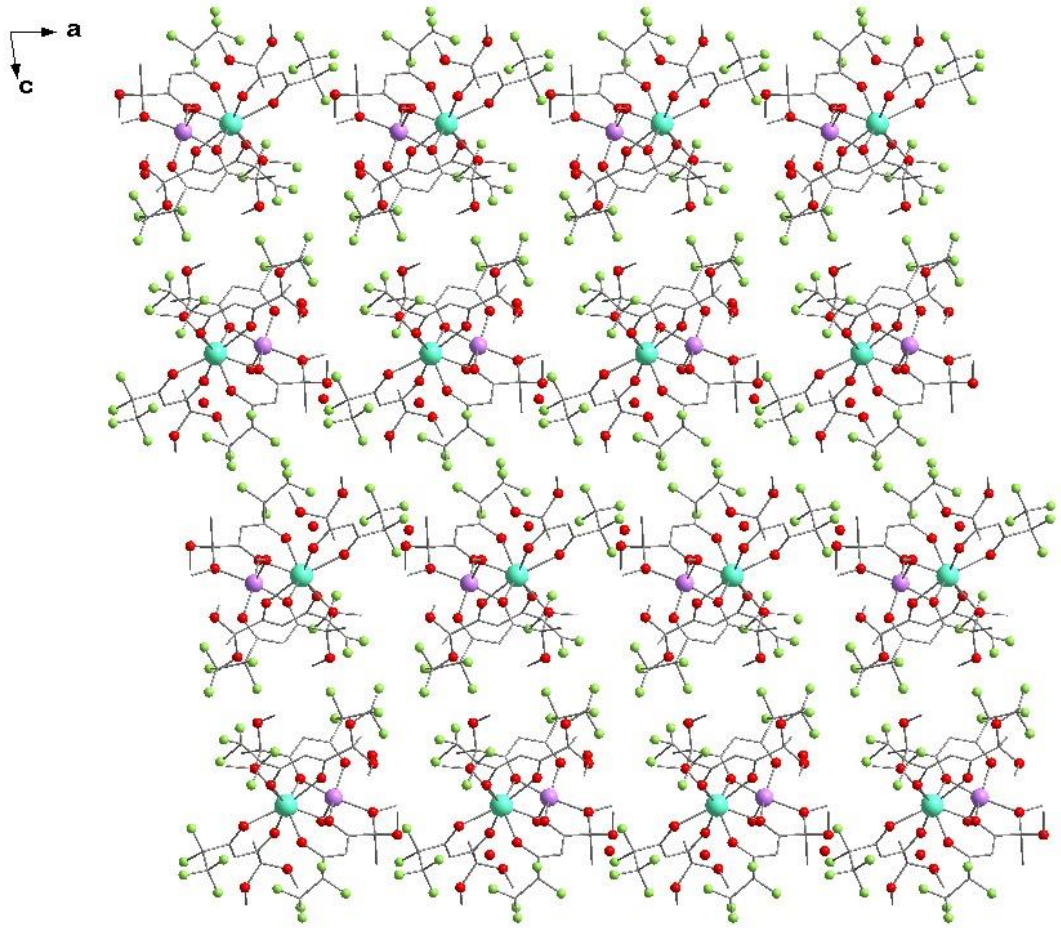

c

Figure S10. Crystal packing of C_2F_5-containing [Ln-Li] β-diketonates **5**-**8** along *c* (**a**), *a* (**b**) and *b* (**c**) axis.

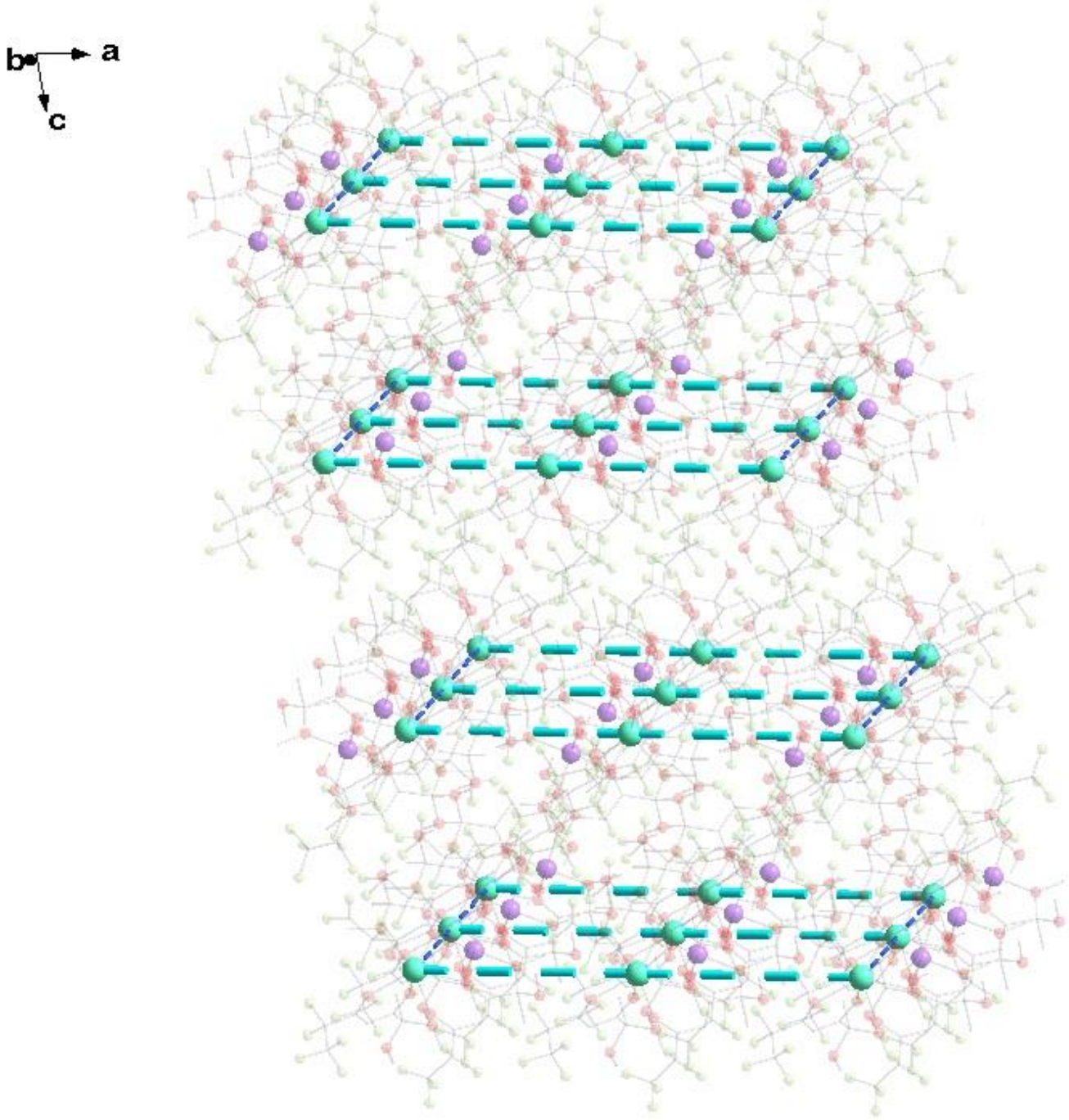

Figure S11. 1D chains assembly of C_2F_5-containing [Ln-Li] β-diketonates **5**-**8**. d(Ln…Ln) ~ 11.1 Å (turquoise dashed line), d(Ln…Ln) ~ 11.3-11.5 Å (blue dashed line).

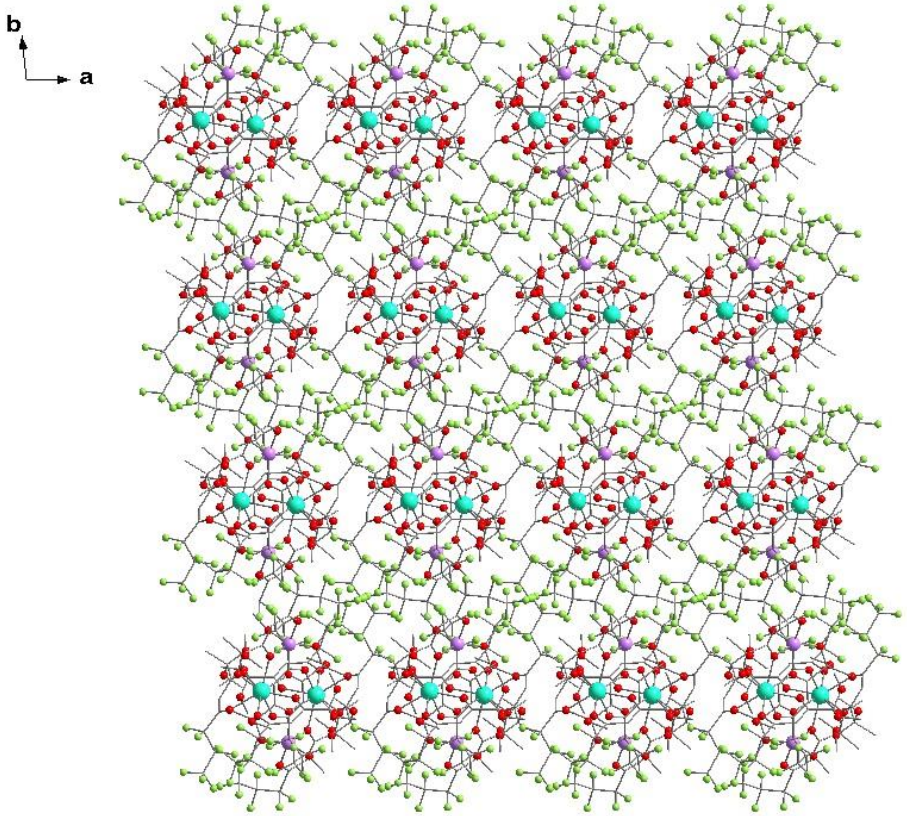

87

a

88

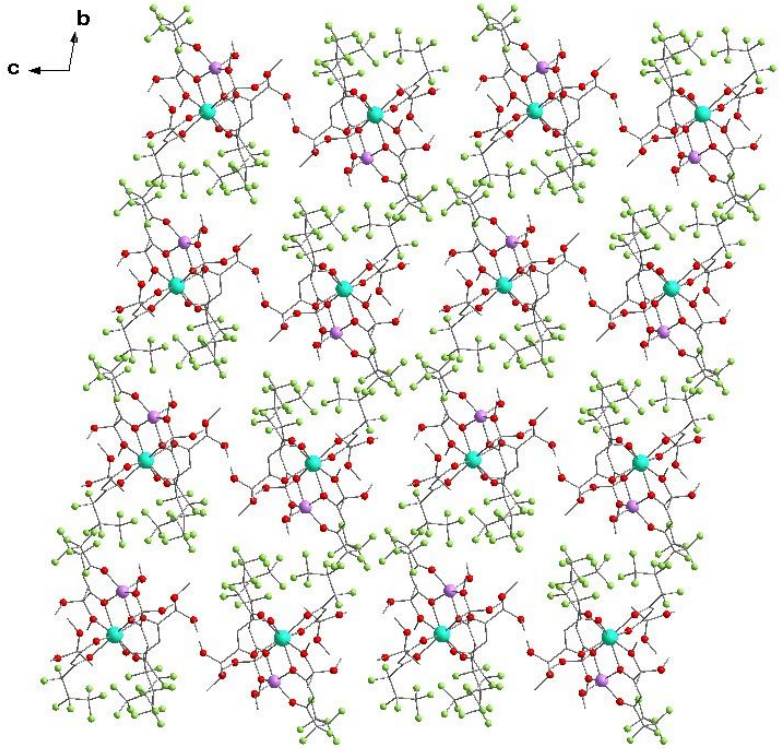

89

b

90

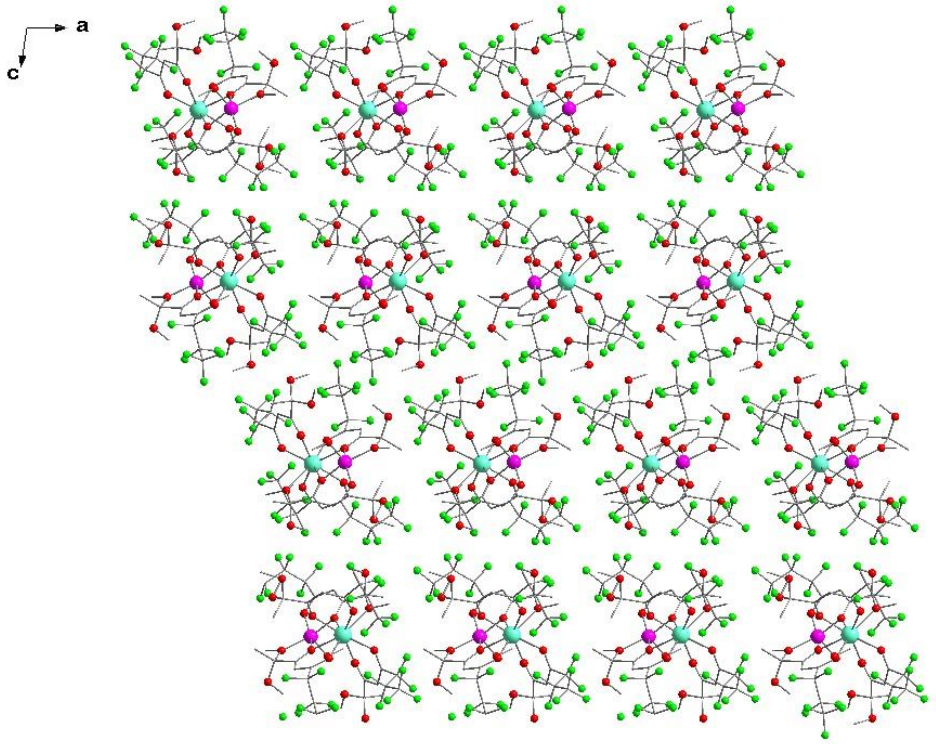

c

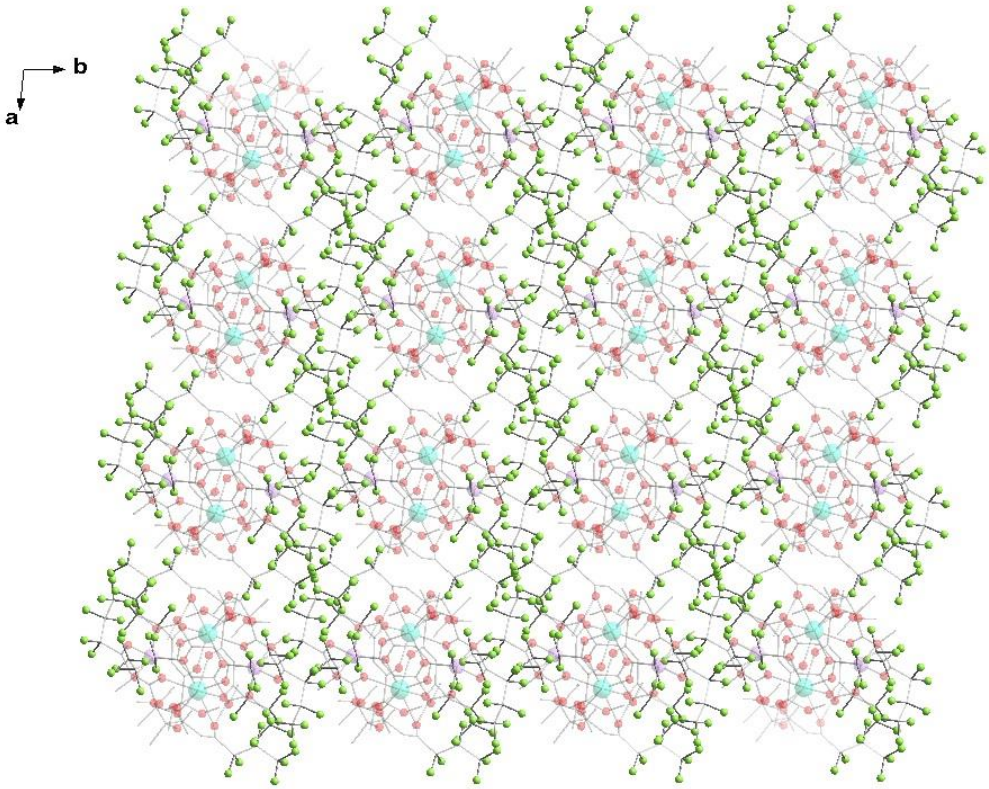

d

Figure S12. Crystal packing of C_3F_7-containing [Ln-Li] β-diketonates **9-11** .

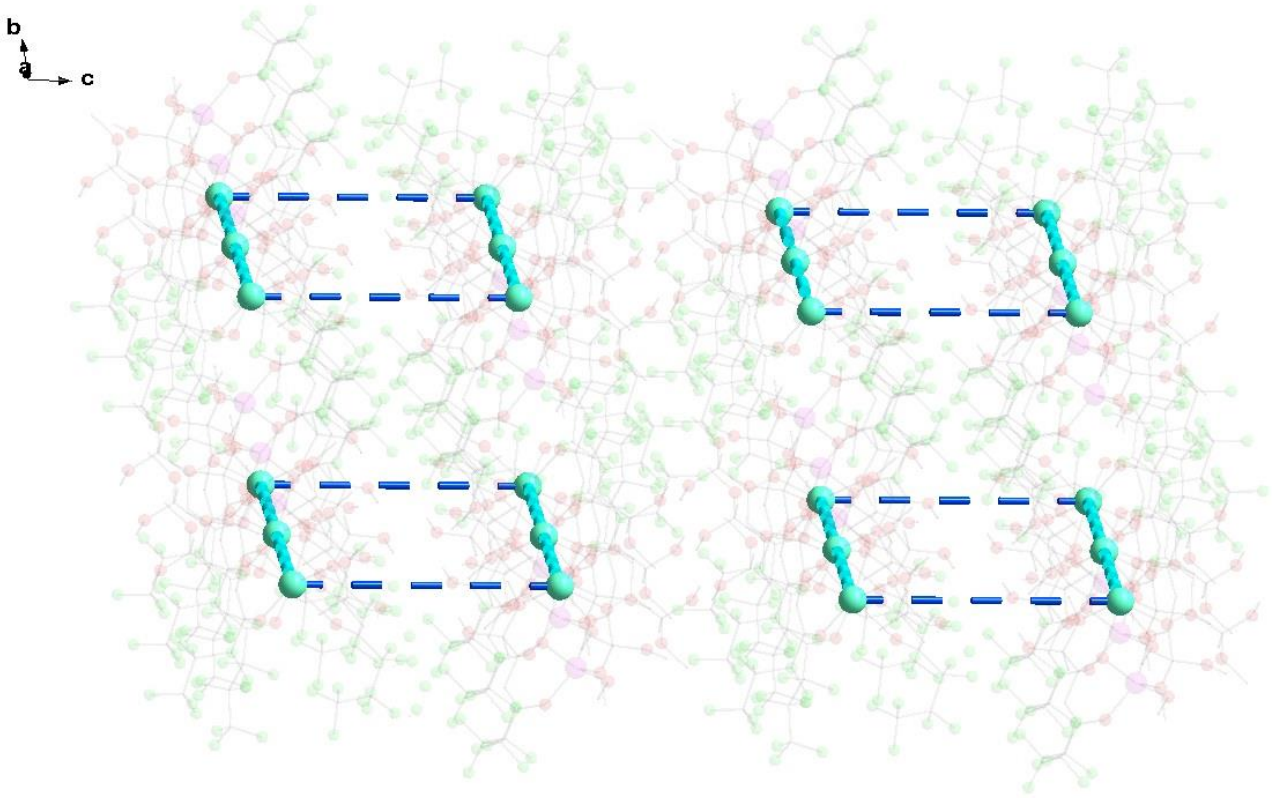

96

Figure S13. Crystal packing of C_3F_7-containing [Ln-Li] β-diketonates **9**-**11**. d(Ln…Ln) ~ 10.6 Å (turquoise dashed line), d(Ln…Ln) ~ 11.0-11.5 Å (blue dashed line). 97 98

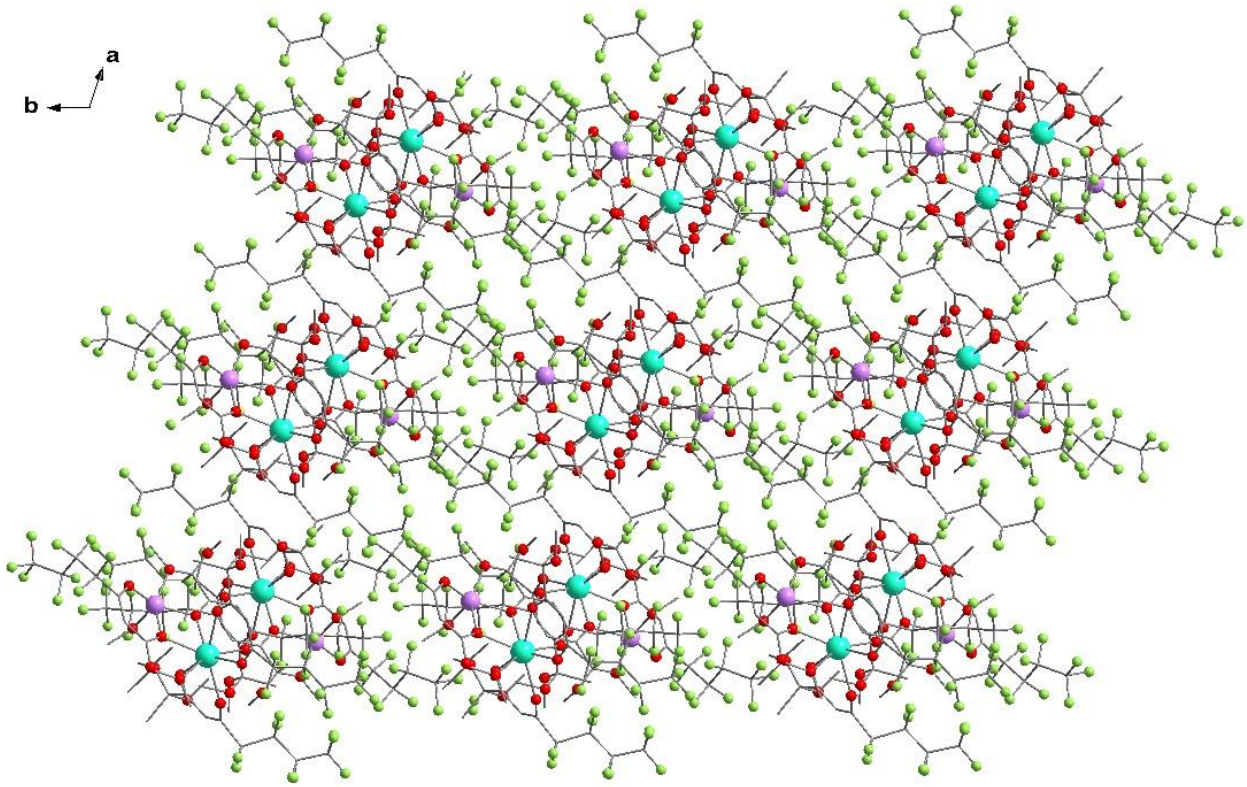

99

a 100

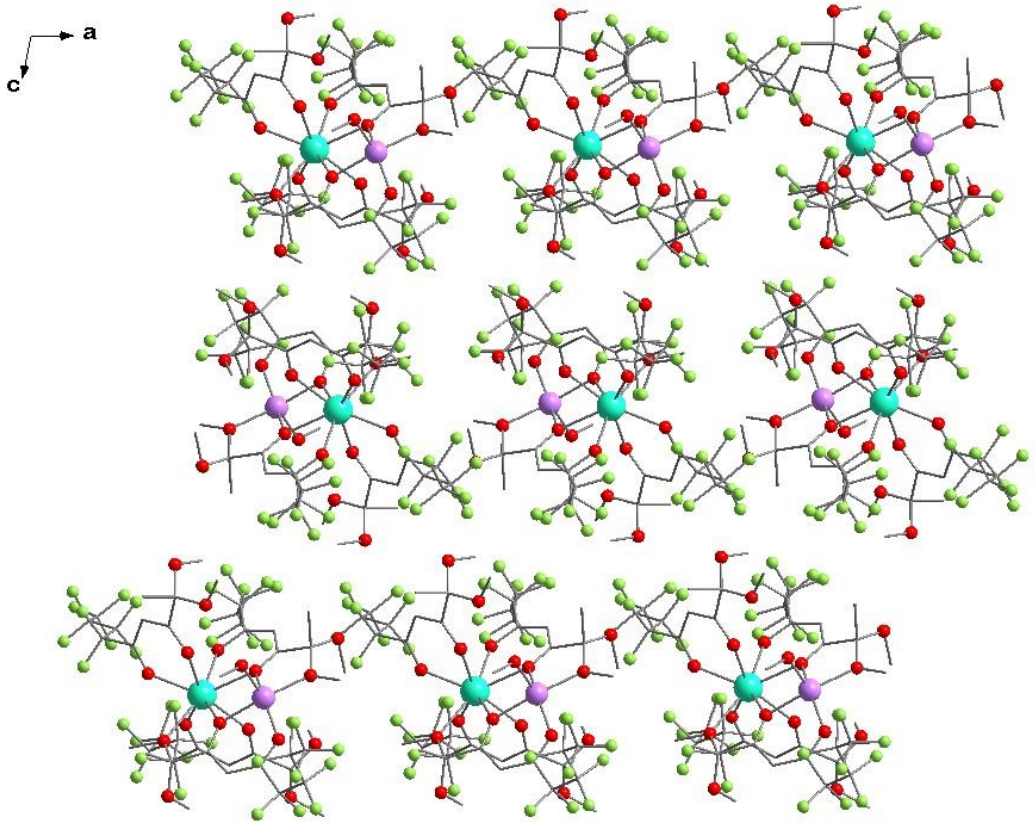

b

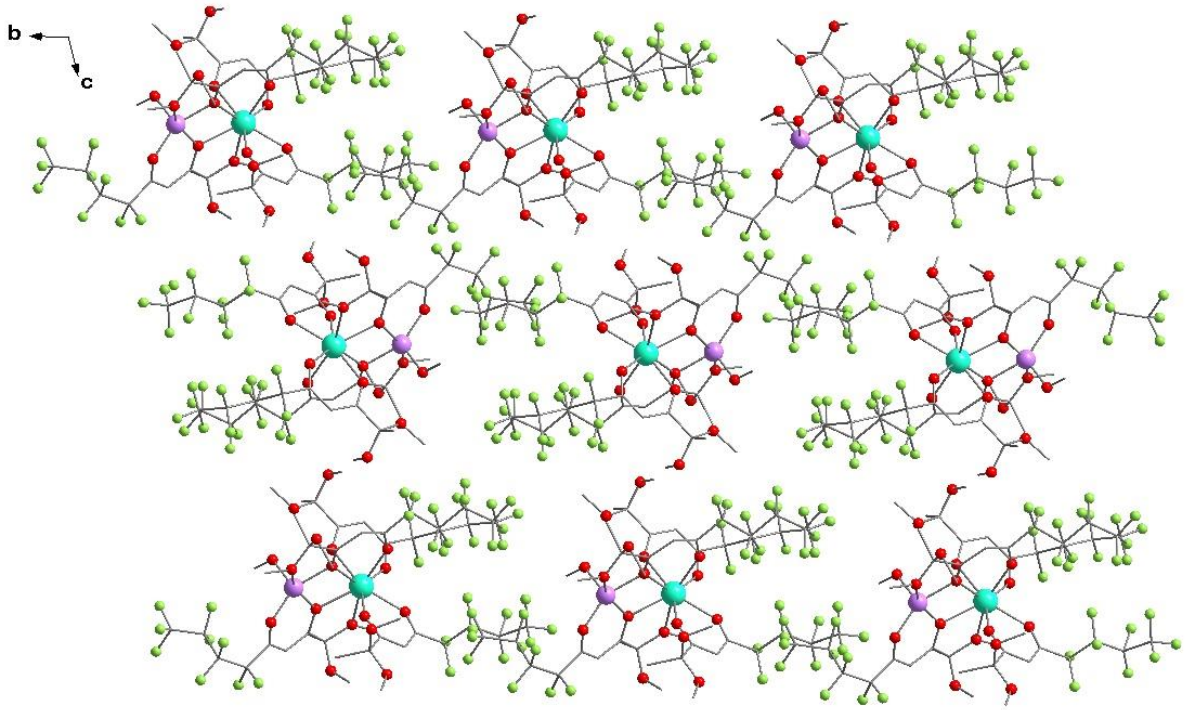

c

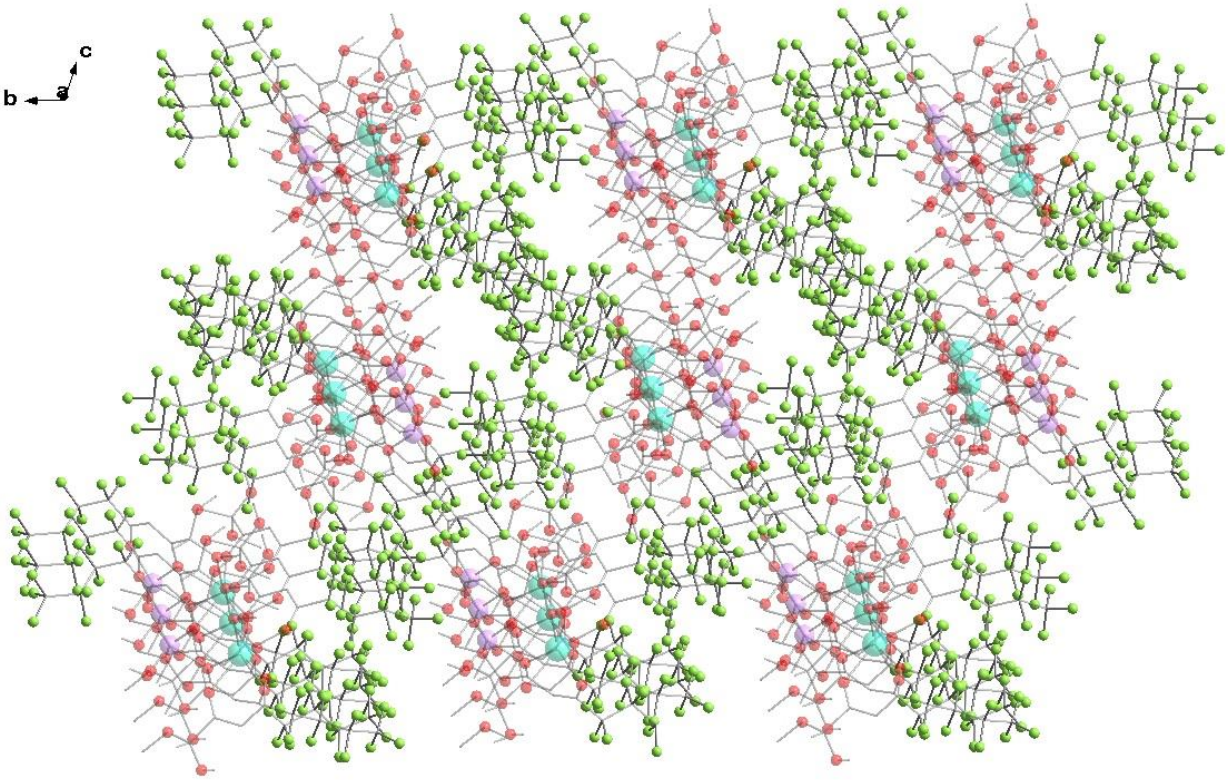

105

d

106

Figure S14. Crystal packing of C_4F_9-containing [Ln-Li] β-diketonates **12**-**15**. 107

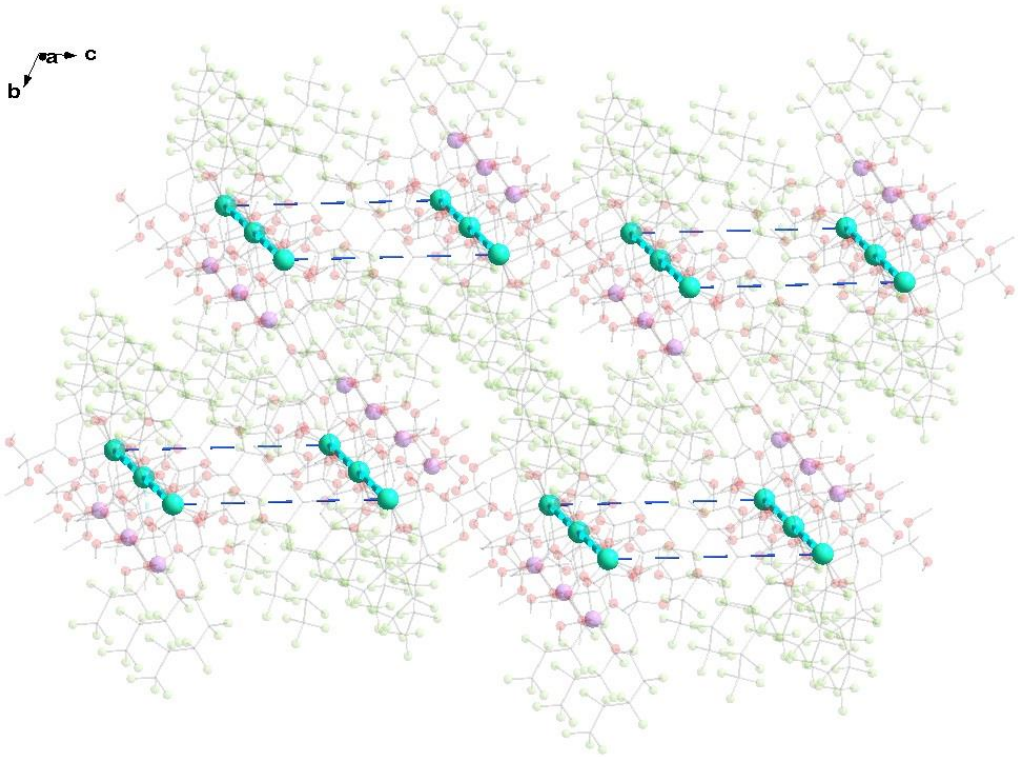

108

Figure S15. Crystal packing of C_4F_9-containing [Ln-Li] β-diketonates **12**-**15**. d(Ln...Ln) ~ 10.7 Å (turquoise dashed line), d(Ln…Ln) ~ 11.1 Å (blue dashed line). 109 110

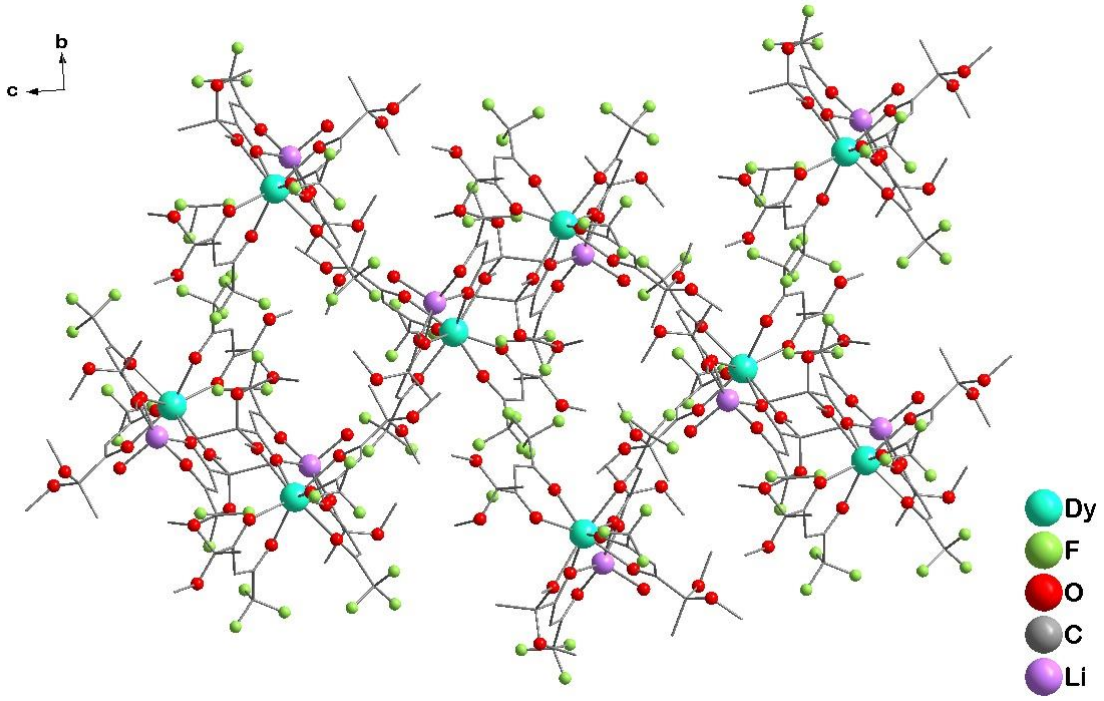

111

a

112

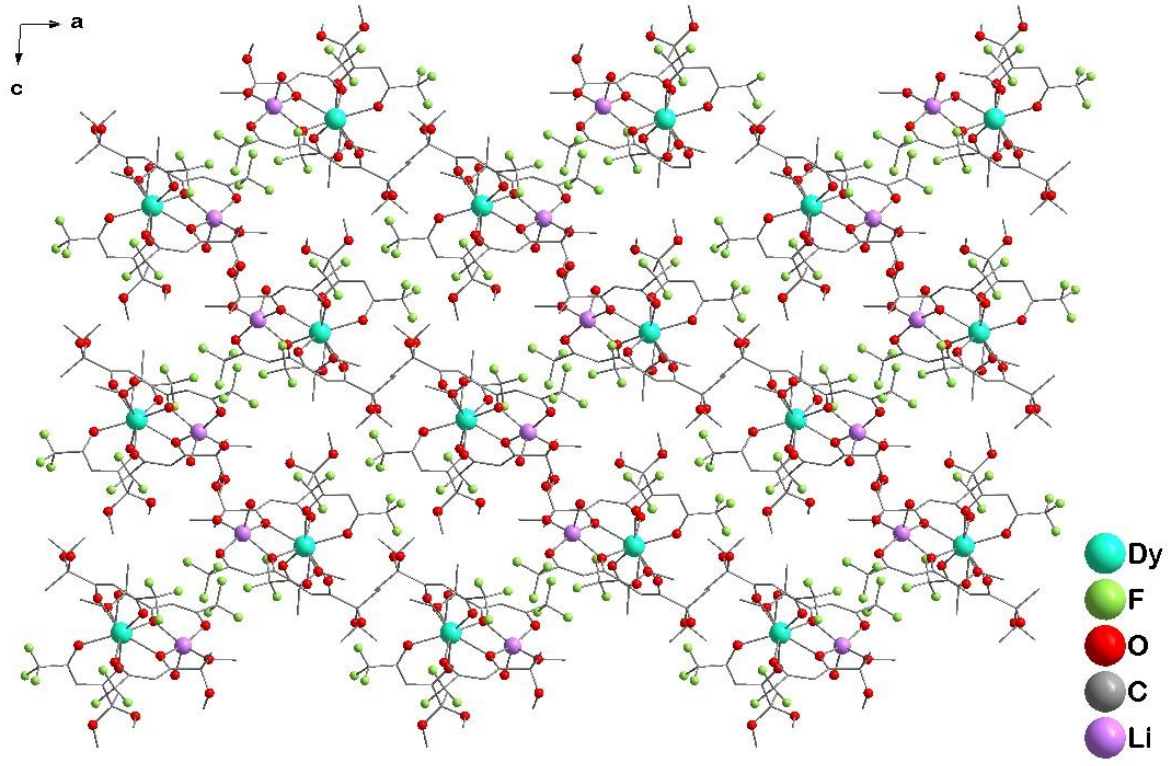

113

b

114

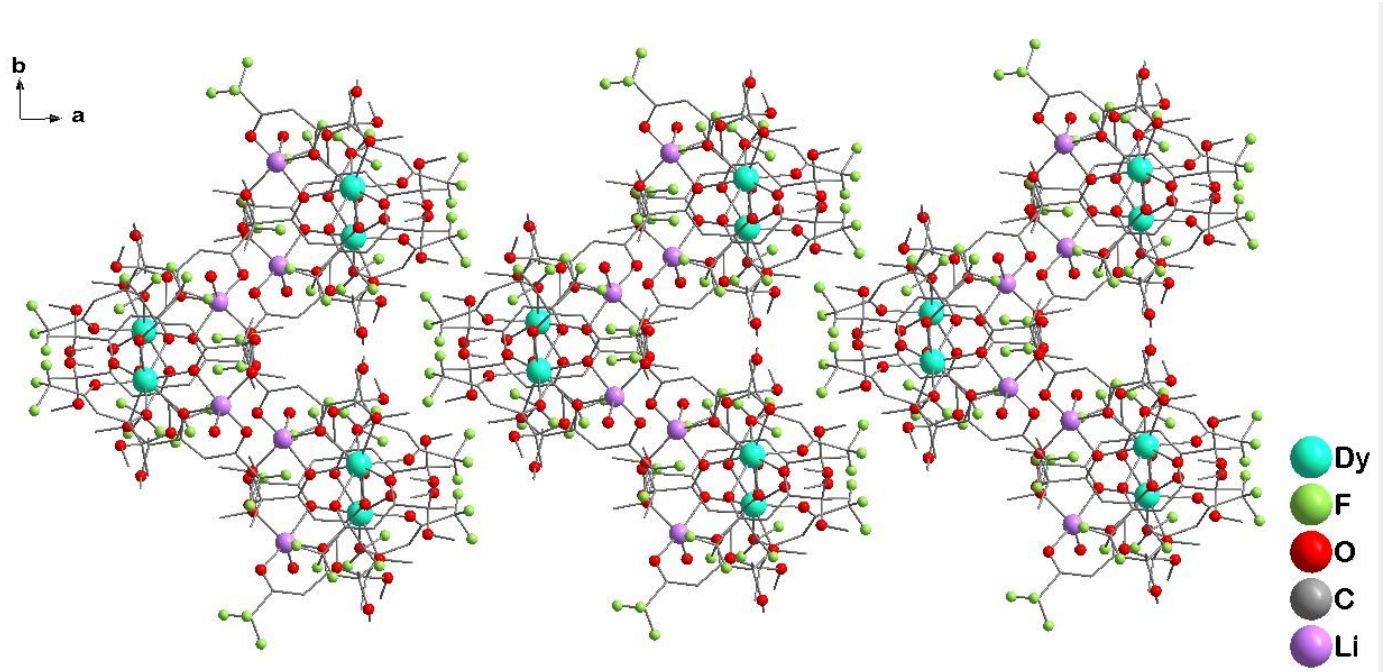

c

Figure S16. Crystal packing of trifluoromethylated [Dy-Li] β-diketonate **16** along *a* (**a**), *b* (**b**) and *c* (**c**) axis.

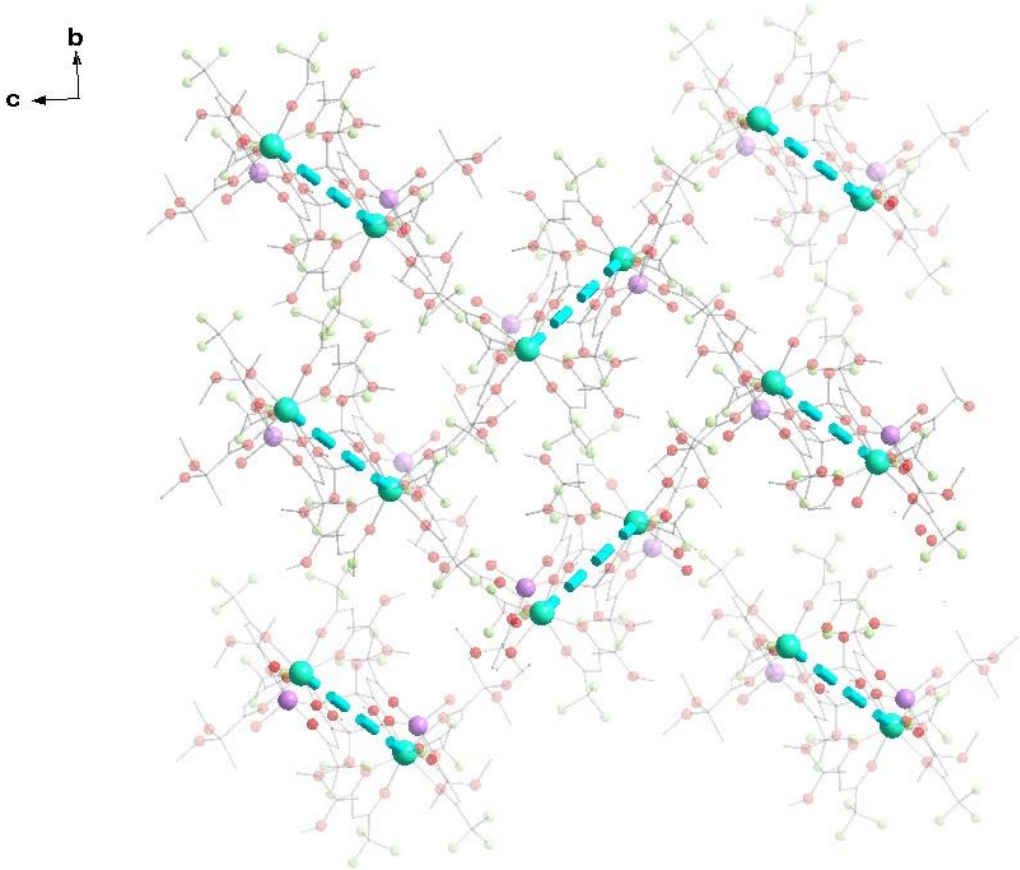

a

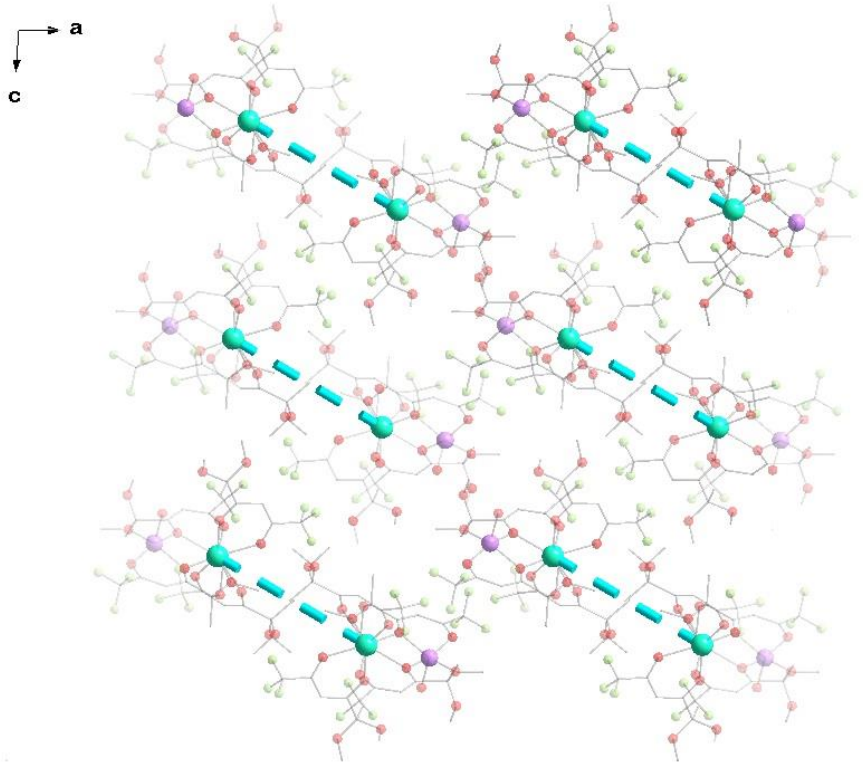

b

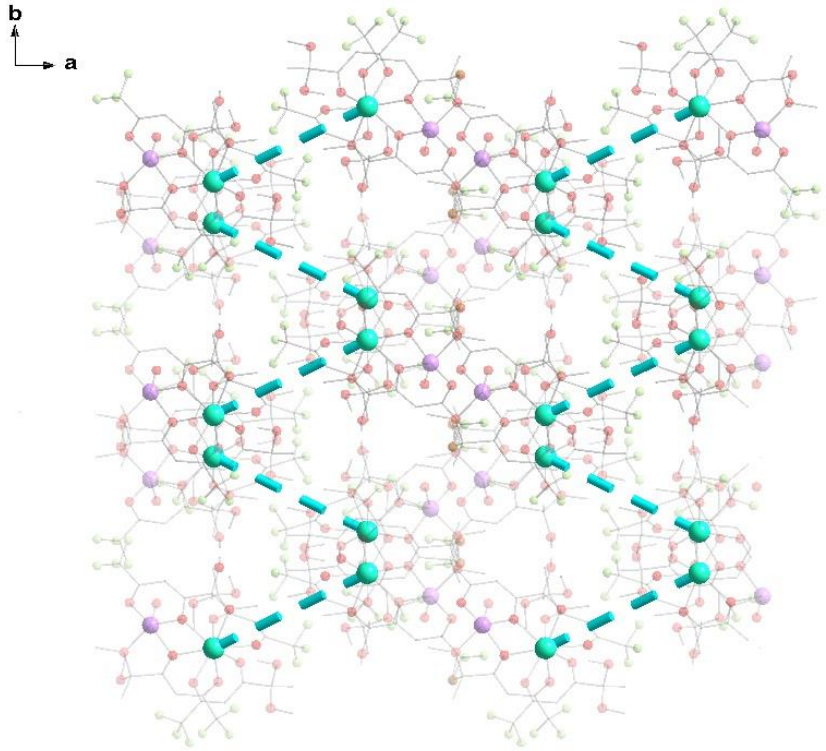

c

Figure S17. Crystal packing of [Dy-Li] CF_3-β-diketonate **16** with the shortest Ln…Ln distance = 9.633(3)Å along *a* (**a**), *b* (**b**) and *c* (**c**) axis (dashed line).

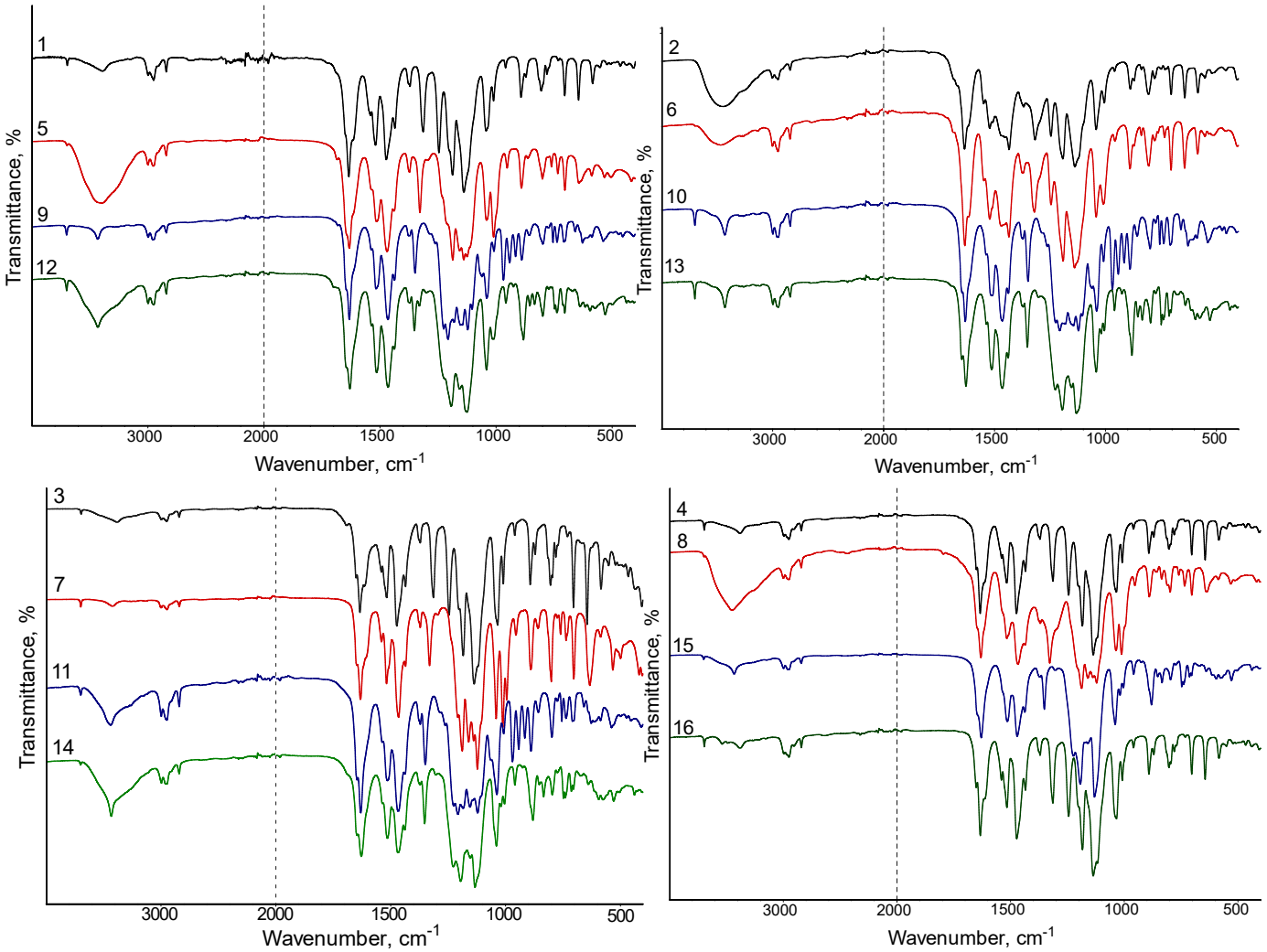

Figure S18. FT-IR spectra of [Ln-Li] R^F-β-diketonates **1-16**.

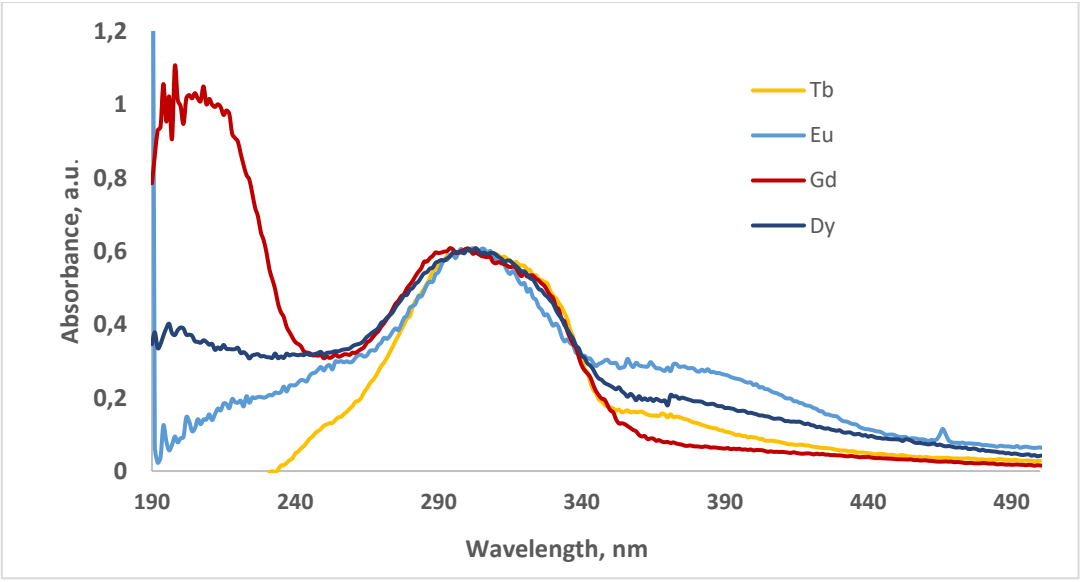

Figure S19 UV-VIS spectra of **1-4** complexes.

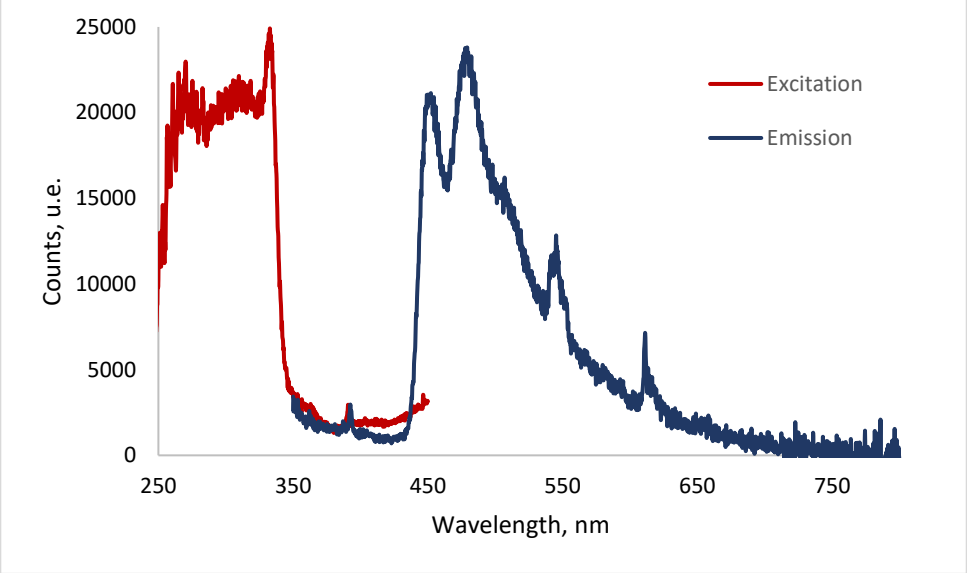

Figure S20. PL excitation and phosphorescence spectra for compound **2** at 77 K.

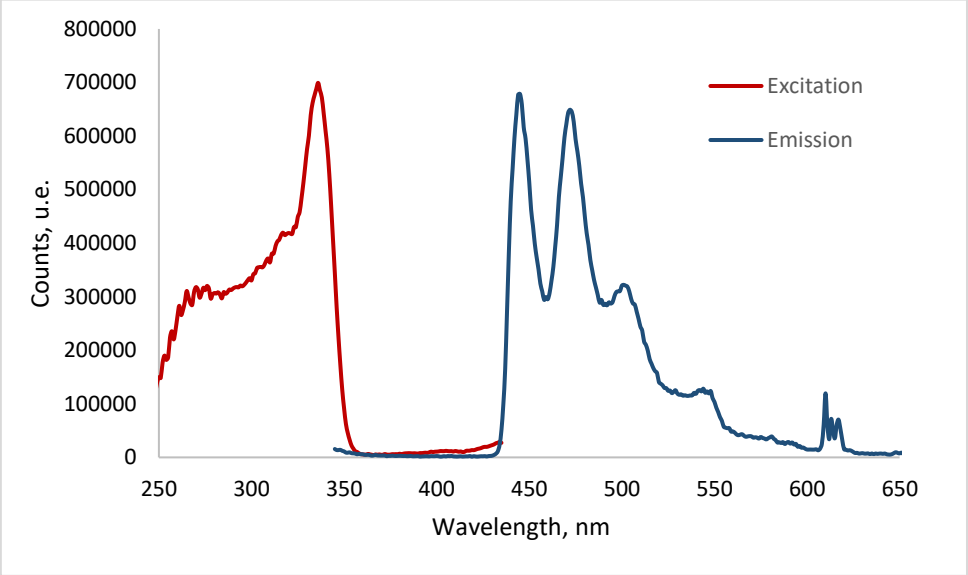

Figure S21. PL excitation and phosphorescence spectra for compound **6** at 77 K.

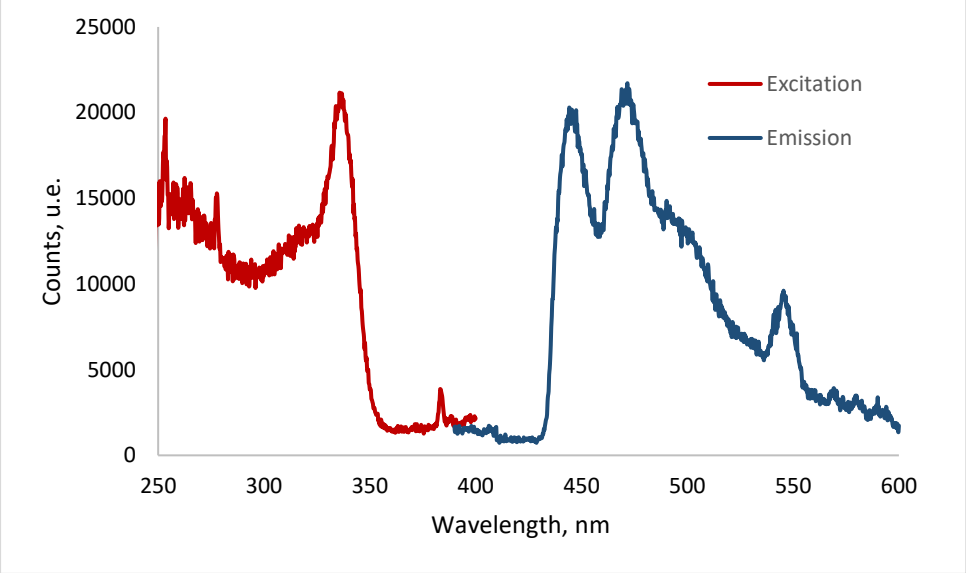

Figure S22. PL excitation and phosphorescence spectra for compound **10** at 77 K.

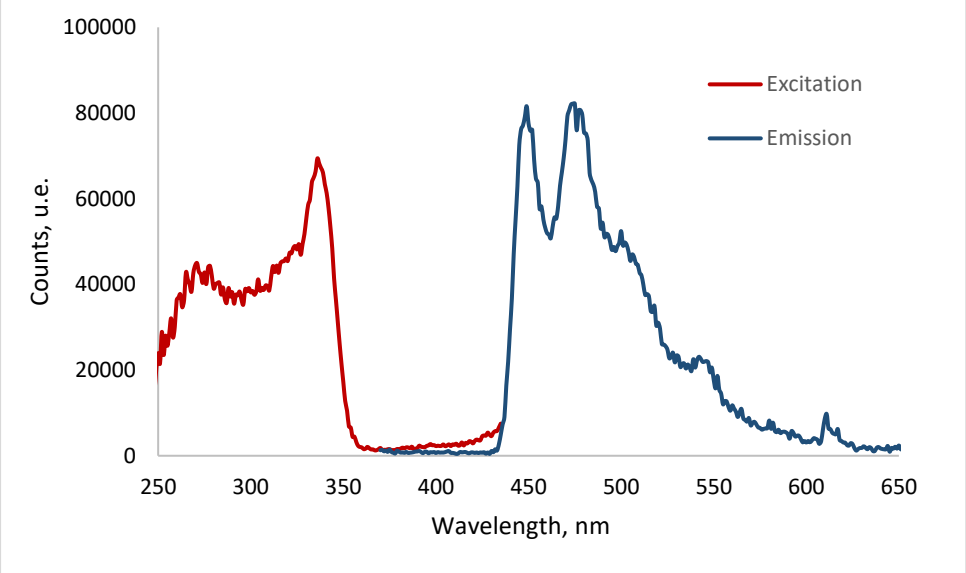

Figure S23. PL excitation and phosphorescence spectra for compound **13** at 77 K.

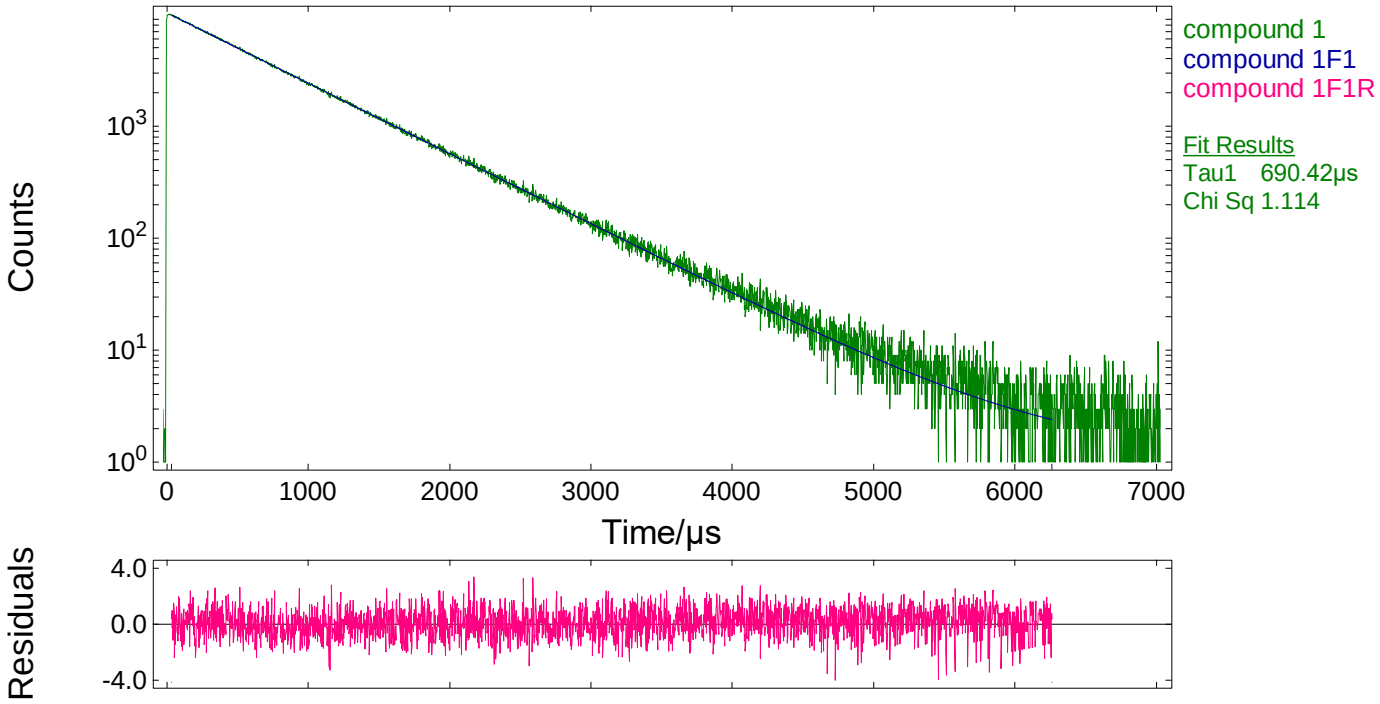

Figure S24. Photoluminescence decay for complex **1** in solid state in the visible spectral range at room temperature.

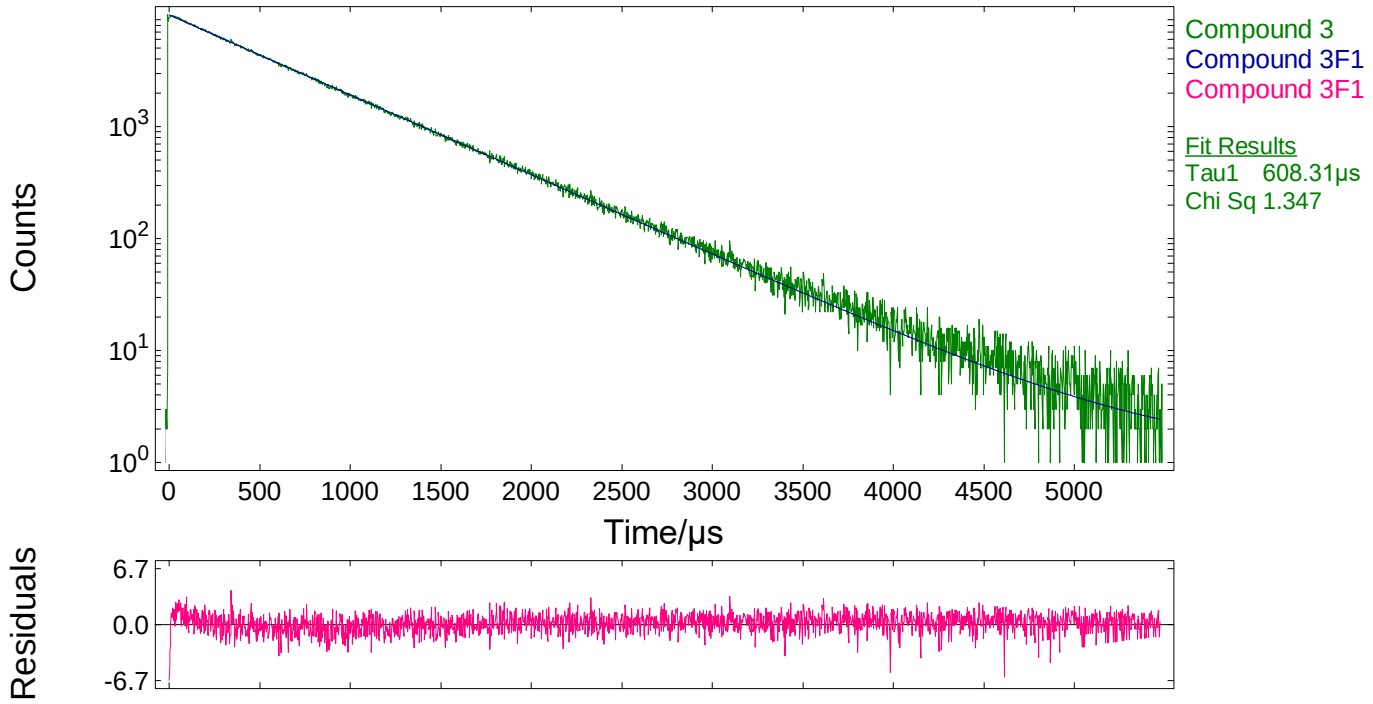

Figure S25. Photoluminescence decay for complex **3** in solid state in the visible spectral range at room temperature.

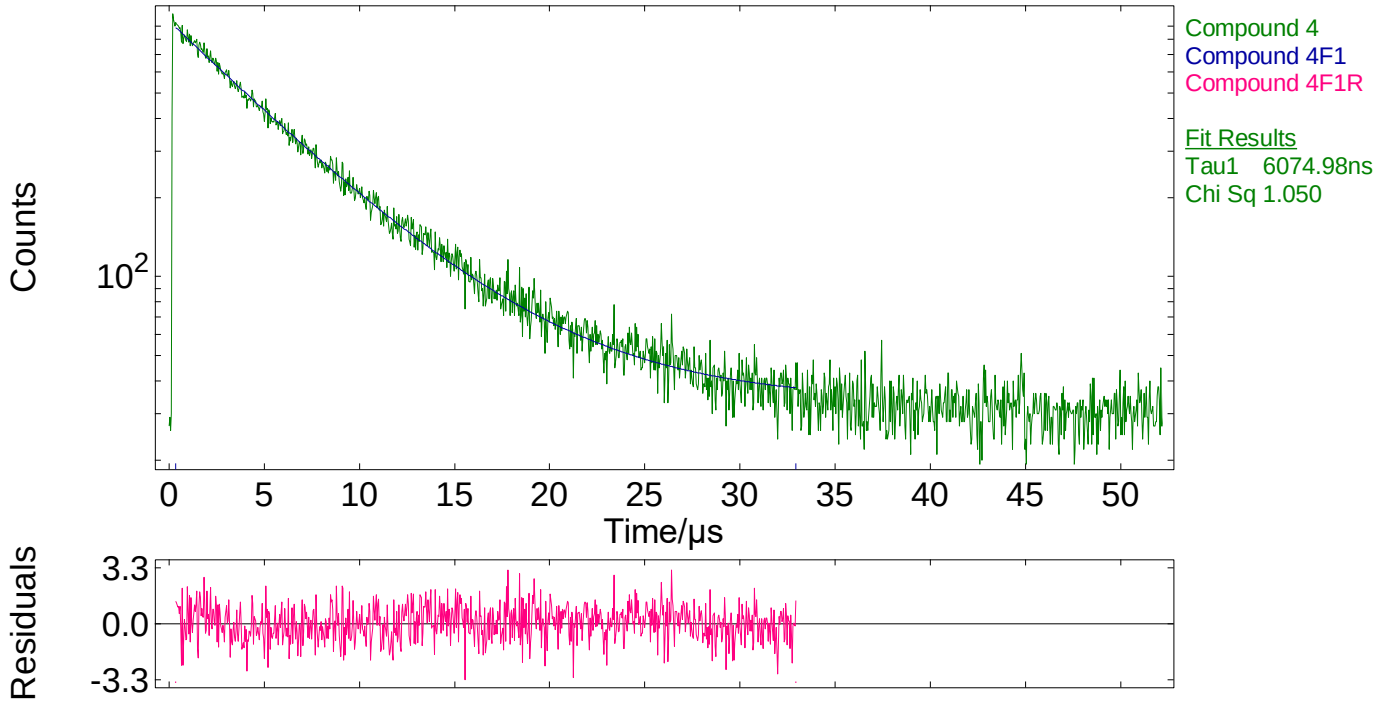

Figure S26. Photoluminescence decay for complex **4** in solid state in the visible spectral range at room temperature.

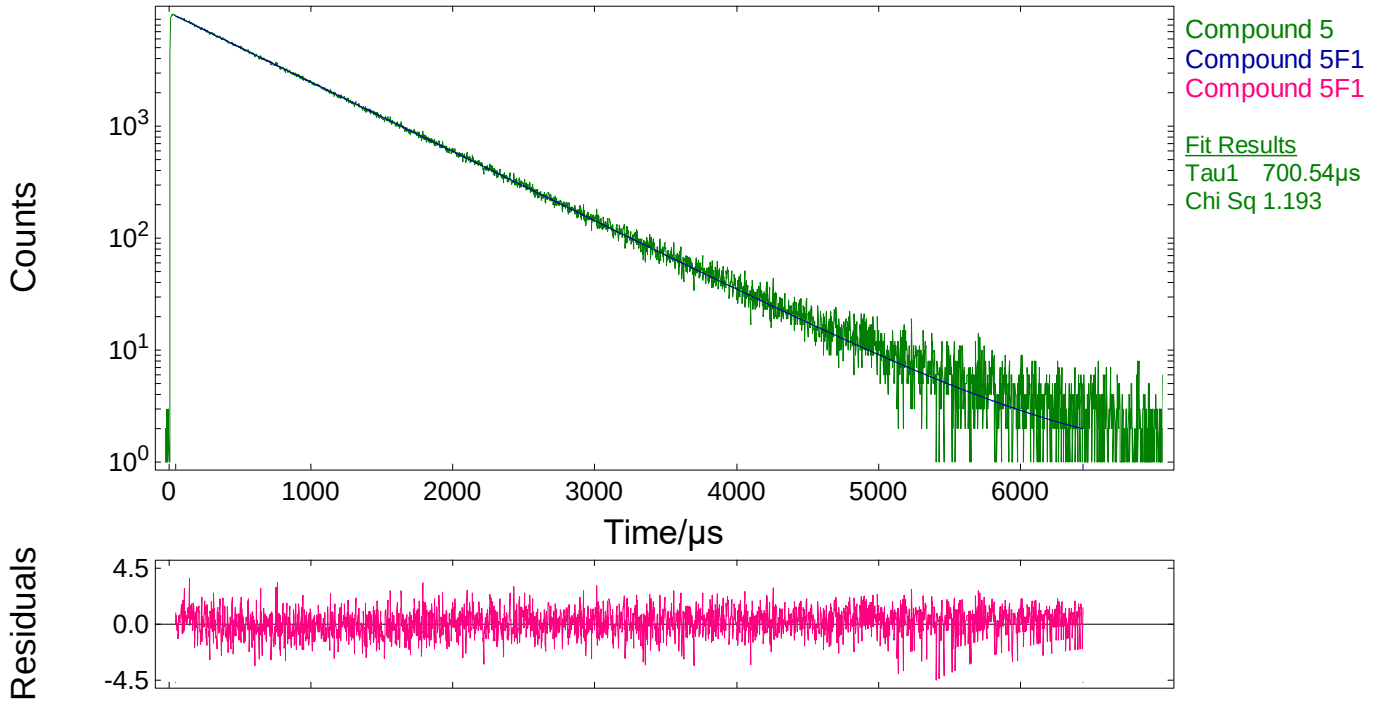

Figure S27. Photoluminescence decay for complex **5** in solid state in the visible spectral range at room temperature.

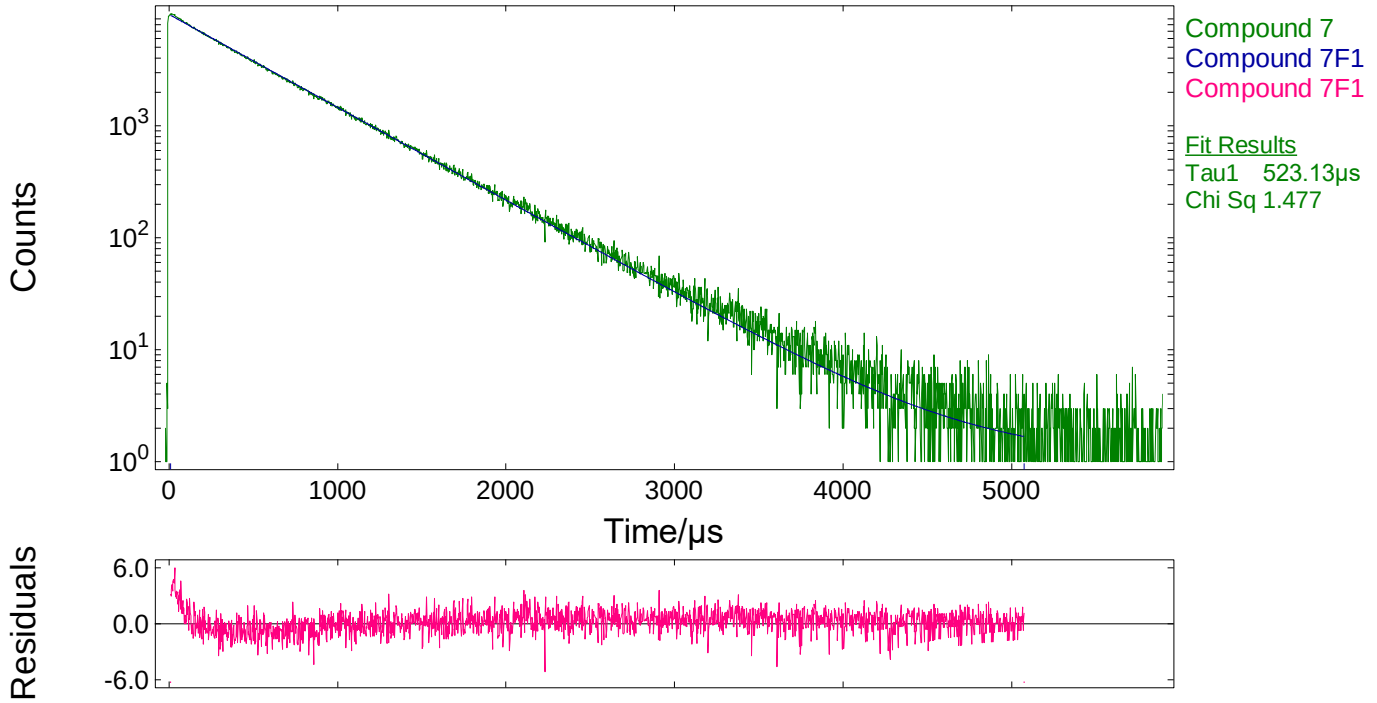

Figure S28. Photoluminescence decay for complex **7** in solid state in the visible spectral range at room temperature.

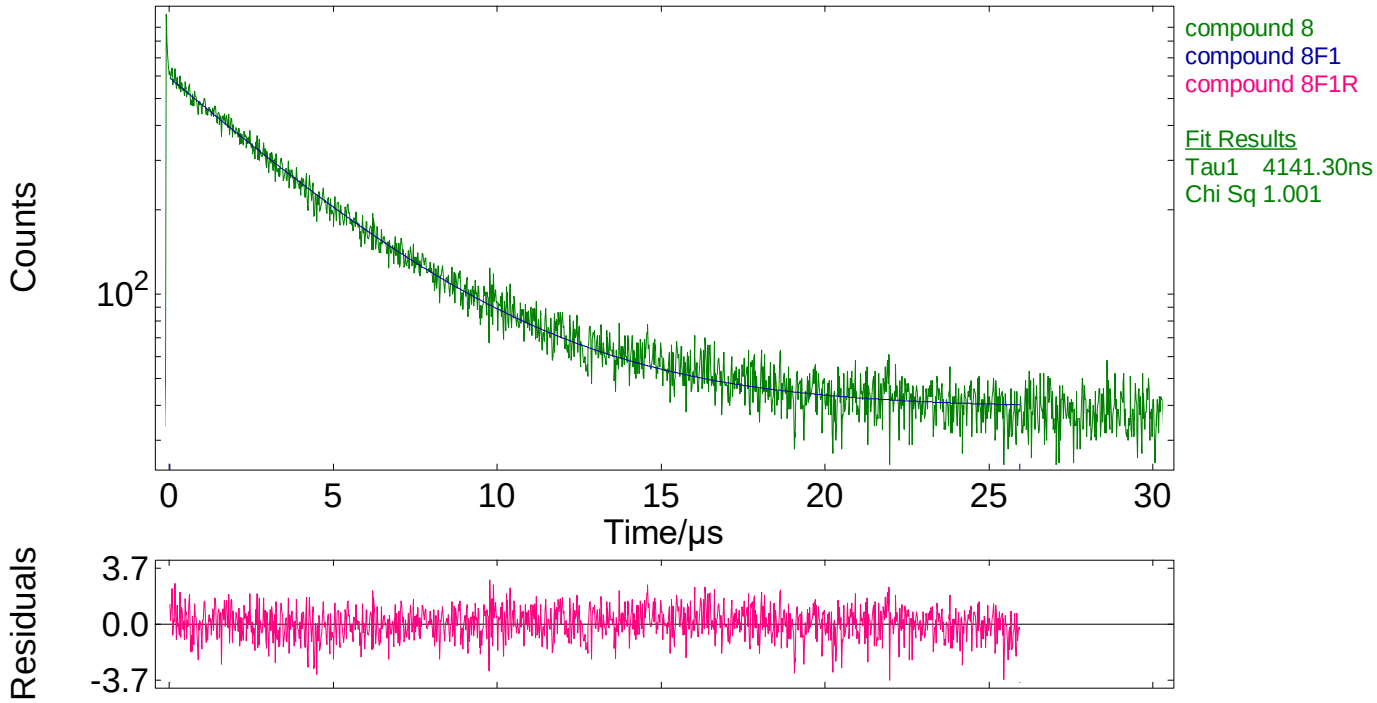

Figure S29. Photoluminescence decay for complex **8** in solid state in the visible spectral range at room temperature.

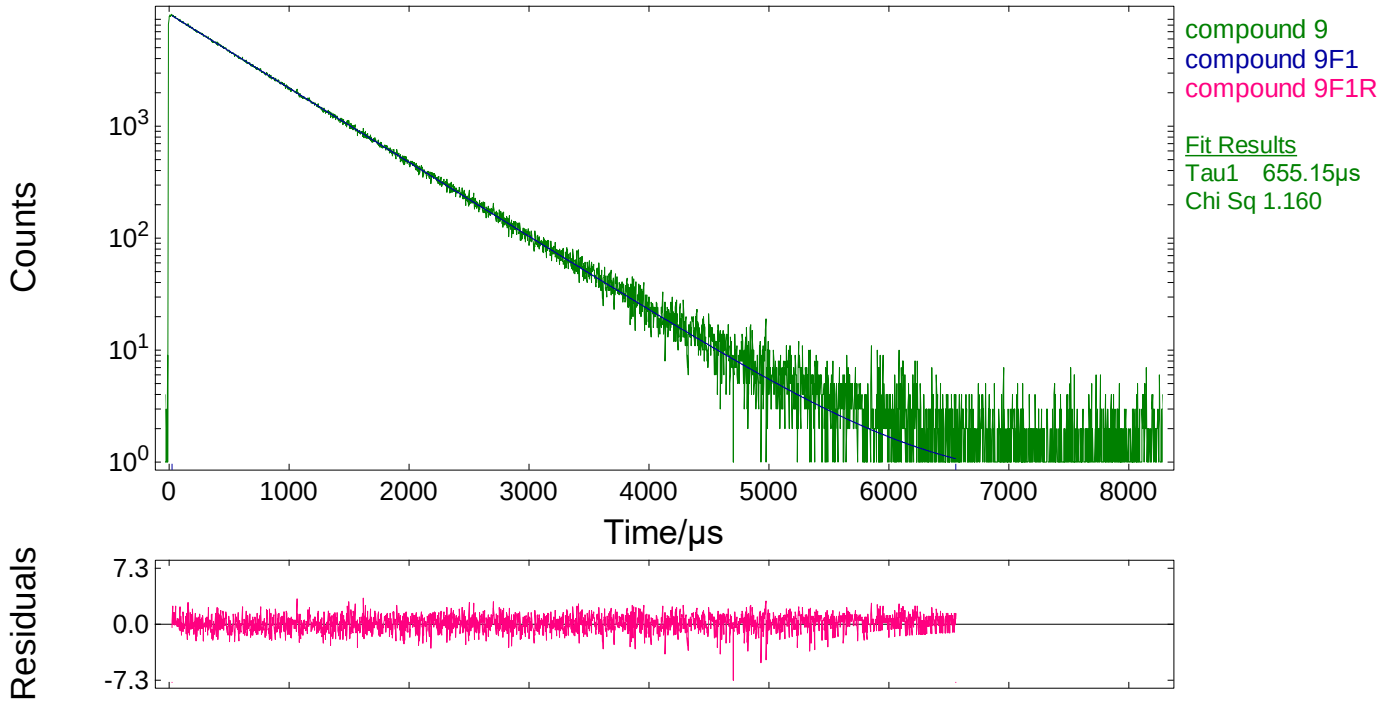

Figure S30. Photoluminescence decay for complex **9** in solid state in the visible spectral range at room temperature.

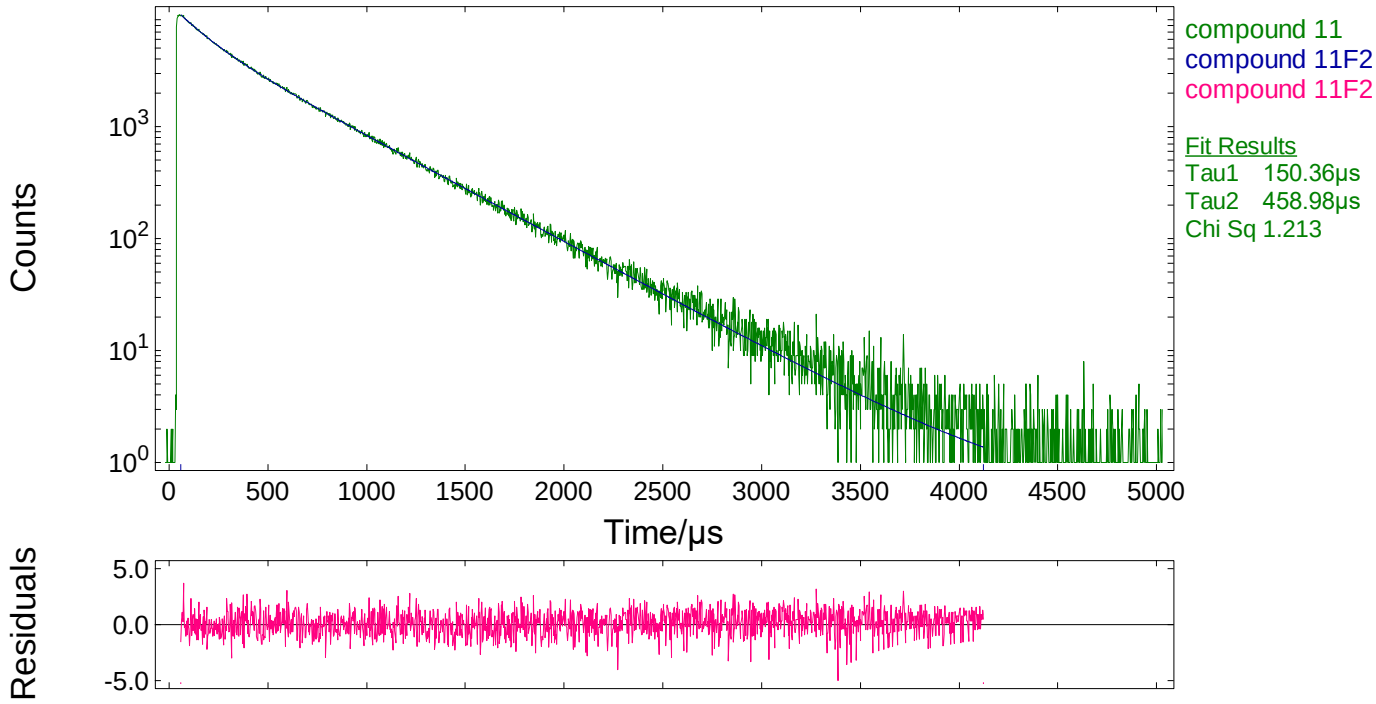

Figure S31. Photoluminescence decay for complex **11** in solid state in the visible spectral range at room temperature.

.

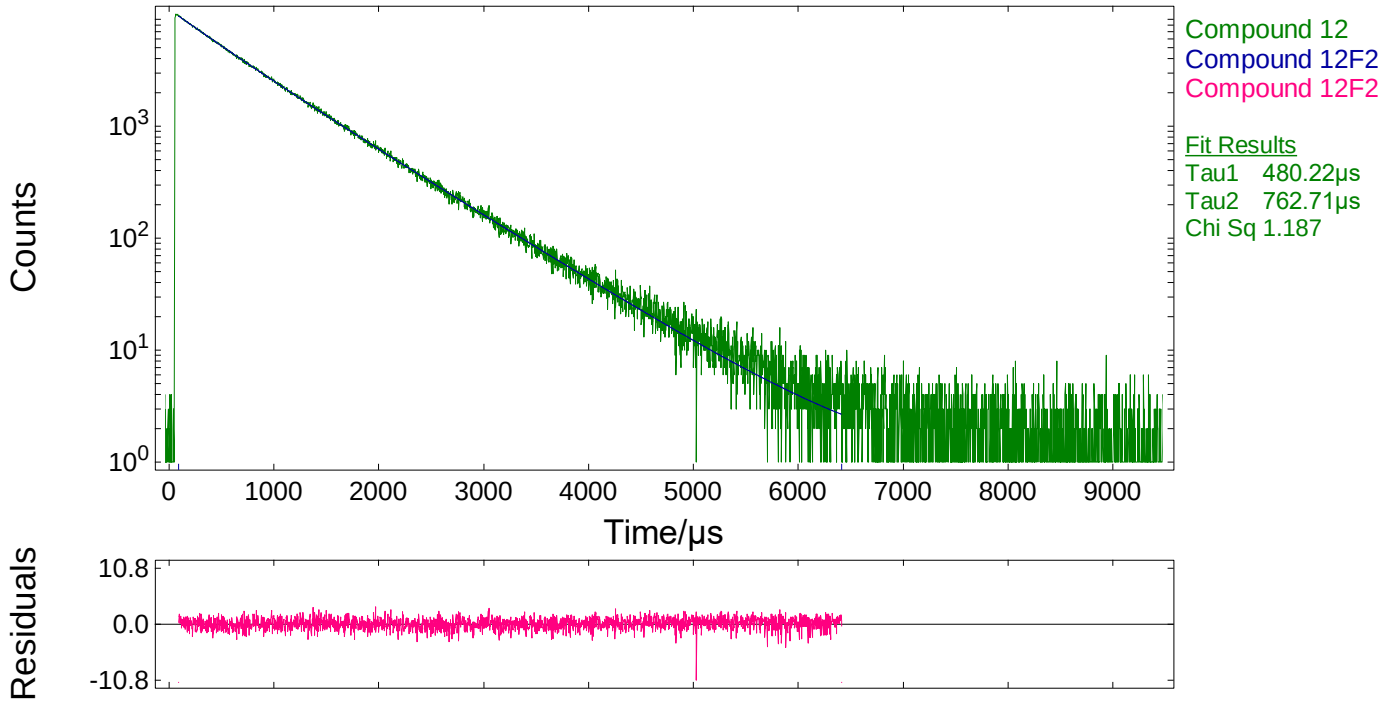

Figure S32. Photoluminescence decay for complex **12** in solid state in the visible spectral range at room temperature.

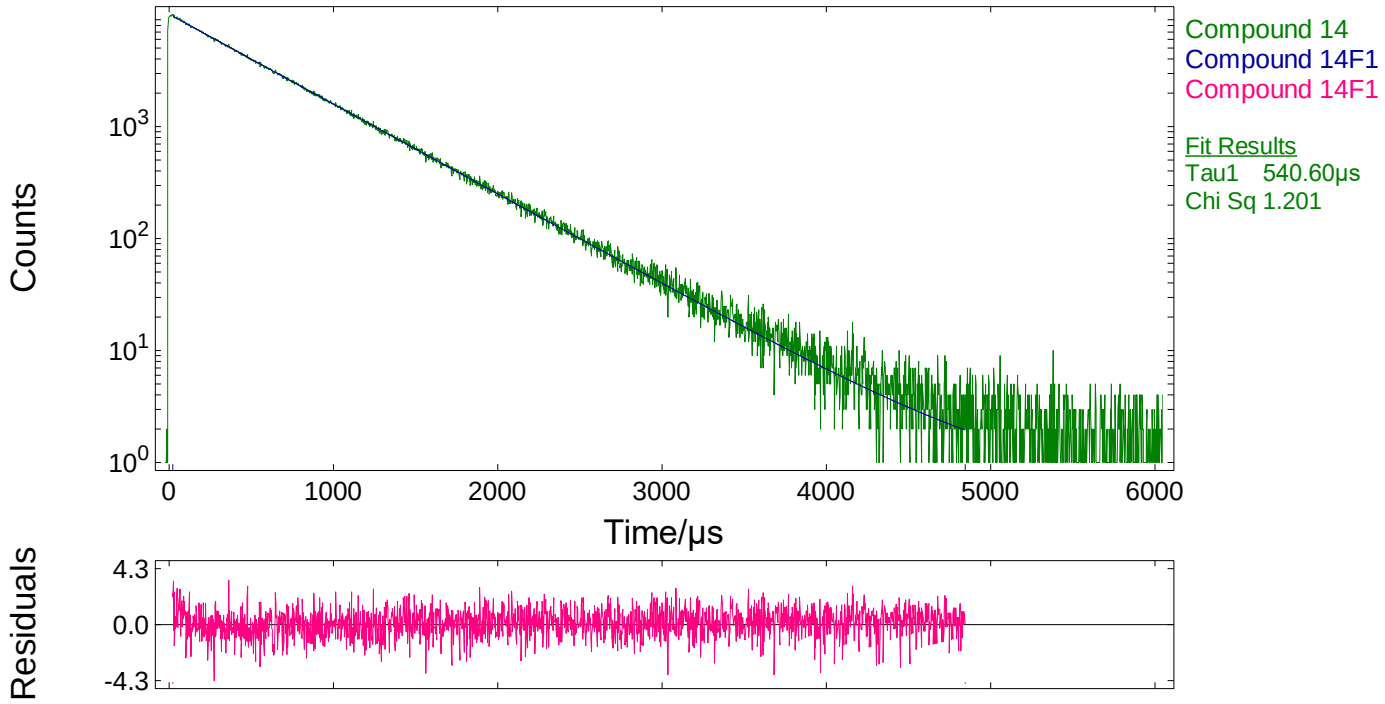

Figure S33. Photoluminescence decay for complex **14** in solid state in the visible spectral range at room temperature.

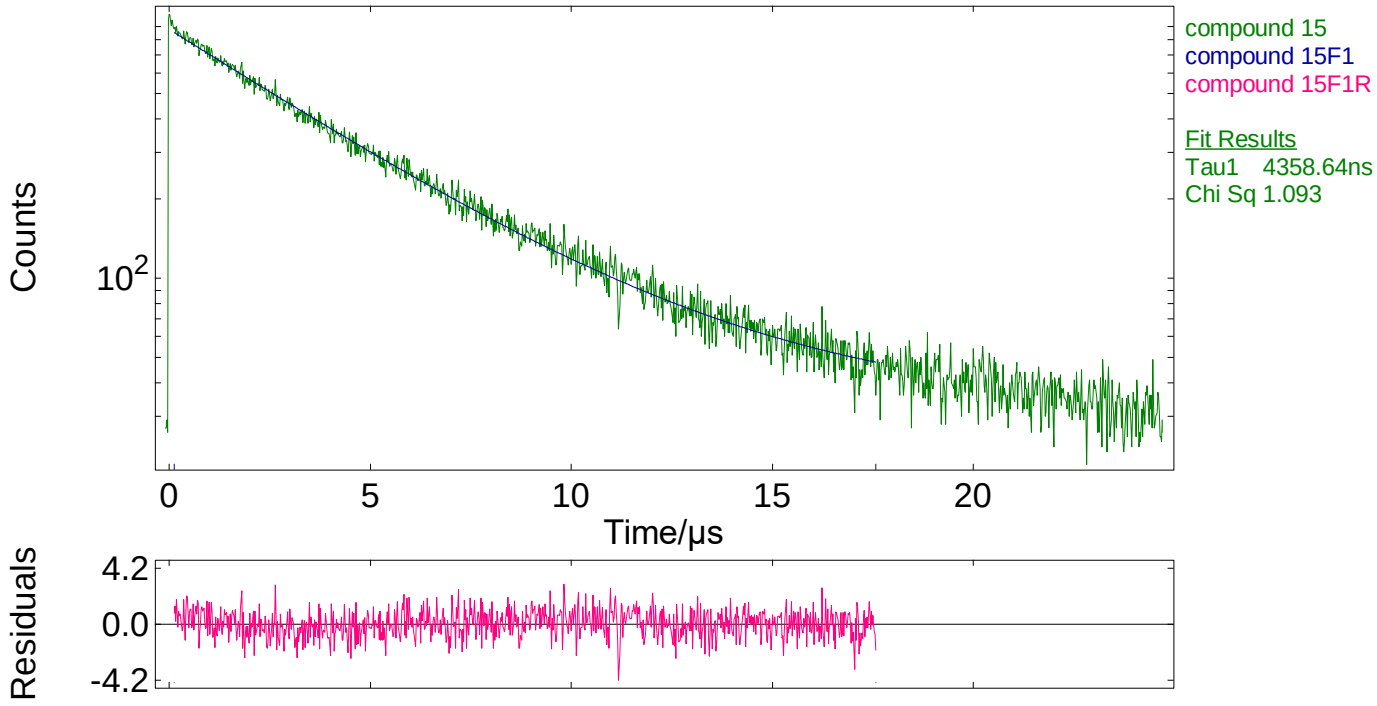

Figure S34. Photoluminescence decay for complex **15** in solid state in the visible spectral range at room temperature.

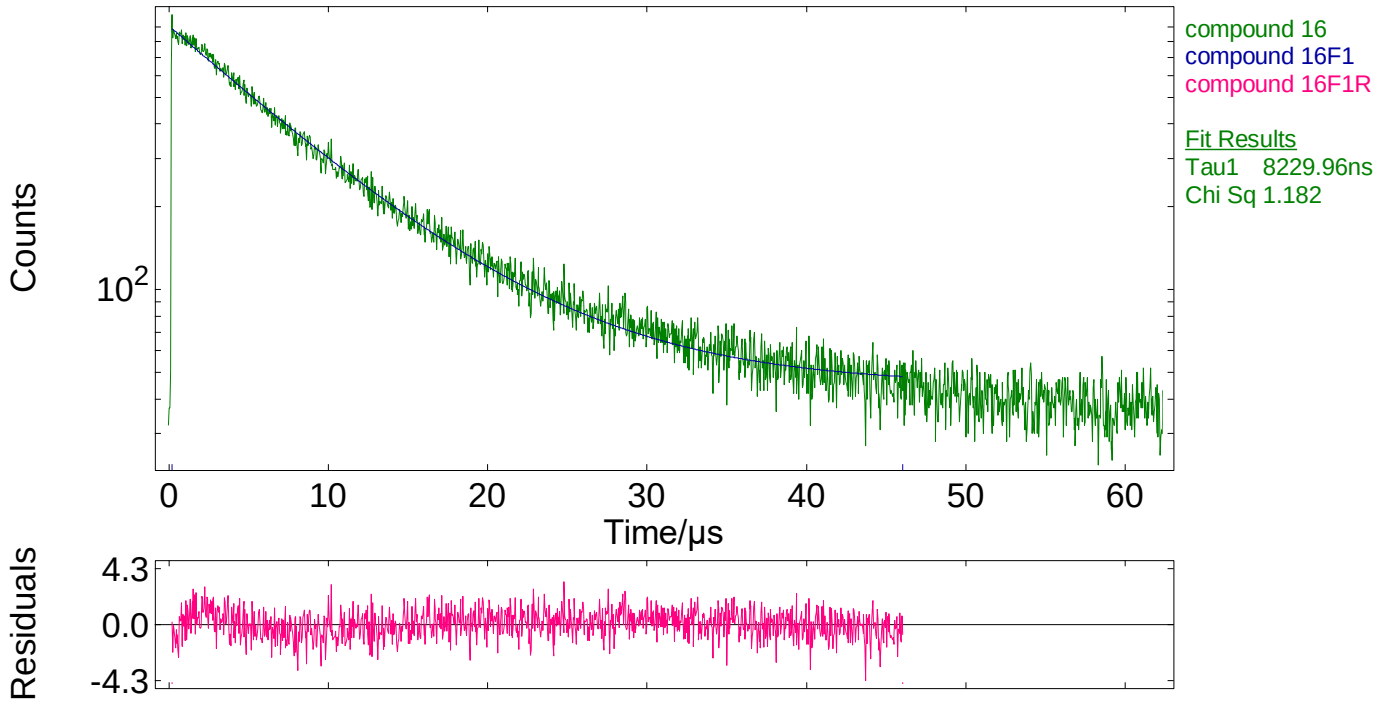

Figure S35. Photoluminescence decay for complex **16** in solid state in the visible spectral range at room temperature.

The AC susceptibility data were fitted using the generalized Debye model:

$$\chi'(\omega) = \chi_S + (\chi_T - \chi_S)\frac{1 + (\omega\tau)^{1-\alpha}\sin\left(\frac{\pi\alpha}{2}\right)}{1 + 2(\omega\tau)^{1-\alpha}\sin\left(\frac{\pi\alpha}{2}\right) + (\omega\tau)^{2-2\alpha}}$$

$$\chi''(\omega) = \chi_T - \chi_S\frac{(\omega\tau)^{1-\alpha}\cos\left(\frac{\pi\alpha}{2}\right)}{1 + 2(\omega\tau)^{1-\alpha}\sin\left(\frac{\pi\alpha}{2}\right) + (\omega\tau)^{2-2\alpha}}$$

Table S15. Temperature dependence of AC susceptibility parameters for **8** at 1000 Oe DC field

H, Oe	T, K	χ_T, cm^3/mol	χ_S, cm^3/mol	τ, s	α
1000	3	4.59(5)	0.136(6)	0.070(2)	0.162(7)
	3.5	3.81(2)	0.124(5)	0.0249(3)	0.122(5)
	4	3.30(1)	0.110(5)	0.01038(9)	0.106(4)
	4.5	2.940(8)	0.096(4)	0.00506(3)	0.094(3)
	5	2.81(5)	0.07(3)	0.003(1)	0.12(2)
	6	2.231(6)	0.076(6)	996(6) ·10^{-6}	0.086(4)
	7	1.918(5)	0.081(9)	444(3) ·10^{-6}	0.078(5)
	8	1.674(3)	0.13(1)	237(3) ·10^{-6}	0.053(5)
	9	1.488(1)	0.16(1)	137(2) ·10^{-6}	0.039(4)
	10	1.31(1)	0.19(8)	84(7) ·10^{-6}	0

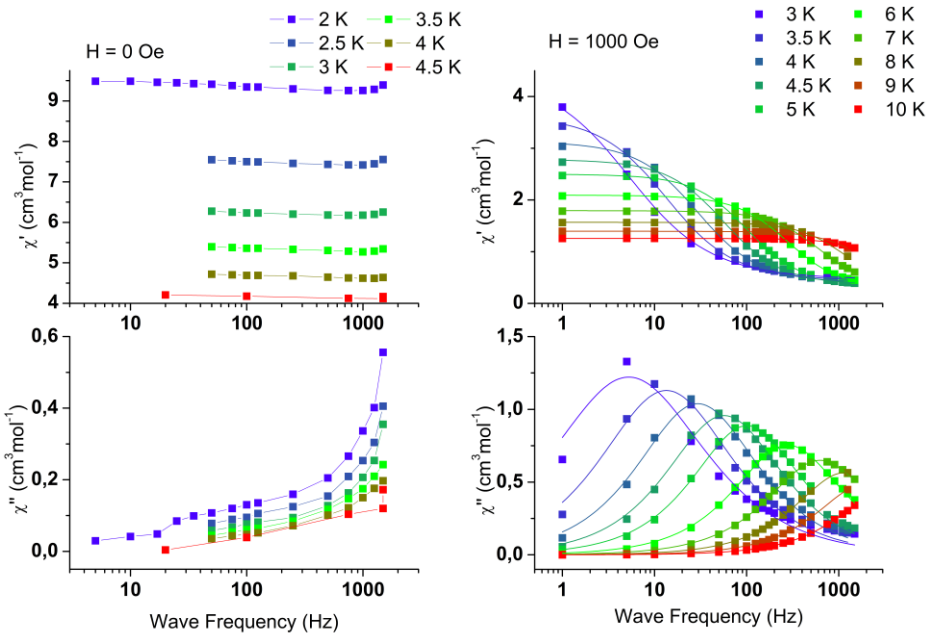

Figure S36 Frequency dependence of the in-phase (χ′) and out-of-phase (χ″) AC magnetic susceptibility for compound **15** under zero (left, points are connected for clarity) and 1000 Oe (right) DC field, solid lines are fits to the Debye model.

Table S16. Temperature dependence of AC susceptibility parameters for **15** at 750 and 1000 Oe DC field

H, Oe	T, K	χ_T, cm^3/mol	χ_S, cm^3/mol	τ, s	α
1000	3	4.5(1)	0.45(2)	0.030(2)	0.30(2)
	3.5	3.64(4)	0.43(2)	0.0118(4)	0.22(1)
	4	3.14(2)	0.39(1)	0.0054(1)	0.175(9)
	4.5	2.78(1)	0.352(8)	0.00279(3)	0.152(6)
	5	2.500(7)	0.35(1)	0.00157(1)	0.121(5)
	6	2.094(4)	0.290(7)	569(4) $\cdot 10^{-4}$	0.113(4)
	7	1.794(3)	0.280(8)	254(2) $\cdot 10^{-4}$	0.097(4)
	8	1.588(1)	0.30(1)	136(2) $\cdot 10^{-4}$	0.072(4)
	9	1.3595(6)	0.31(1)	79(4) $\cdot 10^{-6}$	0.059(3)
	10	1.2562(4)	0.29(1)	47(1) $\cdot 10^{-6}$	0.055(4)

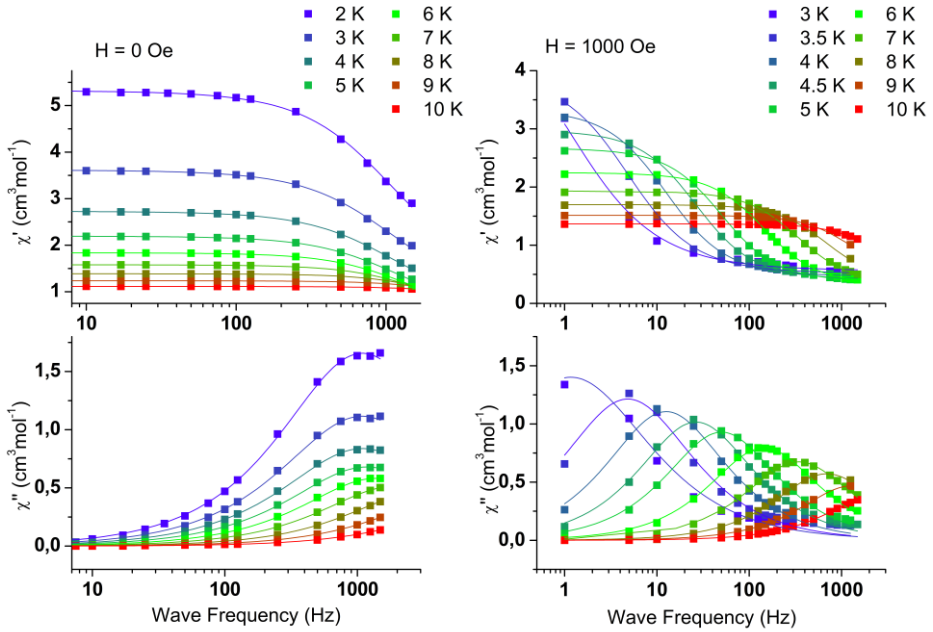

Figure S37 Frequency dependence of the in-phase (χ′) and out-of-phase (χ″) AC magnetic susceptibility for compound **16** under zero (left, points are connected for clarity) and 1000 Oe (right) DC field, solid lines are fits to the Debye model.

Table S17. Temperature dependence of AC susceptibility parameters for **16** at zero and 1000 Oe DC field

H, Oe	T, K	χ_T, cm³/mol	χ_S, cm³/mol	τ, s	α
0	2	5.323(9)	1.21(6)	146(3) ·10⁻⁶	0.135(9)
	3	3.616(6)	0.86(4)	146(3) ·10⁻⁶	0.134(9)
	4	2.729(3)	0.69(2)	145(2) ·10⁻⁶	0.123(5)
	5	2.196(2)	0.58(2)	135(2) ·10⁻⁶	0.107(1)
	6	1.838(1)	0.50(1)	114(1) ·10⁻⁶	0.086(4)
	7	1.5801(6)	0.42(1)	83(1) ·10⁻⁶	0.076(3)
	8	1.3869(4)	0.39(1)	56(1) ·10⁻⁶	0.064(4)
	9	1.2369(4)	0.32(3)	31(1) ·10⁻⁶	0.078(6)
	10	1.1153(6)	0.46(7)	22(3) ·10⁻⁶	0.083(1)
1000	3	5.3(3)	0.56(2)	0.13(2)	0.32(3)
	3.5	3.92(7)	0.51(1)	0.033(2)	0.21(2)
	4	3.35(3)	0.46(1)	0.0126(3)	0.17(1)
	4.5	2.98(2)	0.41(1)	610(1) ·10⁻⁵	0.148(7)
	5	2.67(1)	0.377(7)	318(3) ·10⁻⁵	0.133(6)
	6	2.249(7)	0.326(7)	110(1) ·10⁻⁵	0.121(5)
	7	1.934(5)	0.320(9)	46(1) ·10⁻⁵	0.114(6)
	8	1.698(3)	0.37(1)	23(1) ·10⁻⁵	0.094(6)
	9	1.515(1)	0.45(2)	12(1) ·10⁻⁵	0.081(1)
	10	1.3664(8)	0.48(2)	6(1) ·10⁻⁵	0.082(6)

Field dependence of magnetization for were studied for complexes **8** and **16** and shown in Figures S38 and S39. The field dependencies of magnetization are nol-linear at low temperature and saturates in fields H > 15 kOe at 2 K. The saturation magnetizations at magnetic field of 45 kOe are 5.69 μB for **8** and 5.57 μB for **16** and are lower

than a theoretical value of 10 μ_B for one Dy^{III} ion. The M(H/T) dependencies at different temperatures do not coincide, that imply anisotropy effects take place (Figure S38 *b*, S38 *b*).

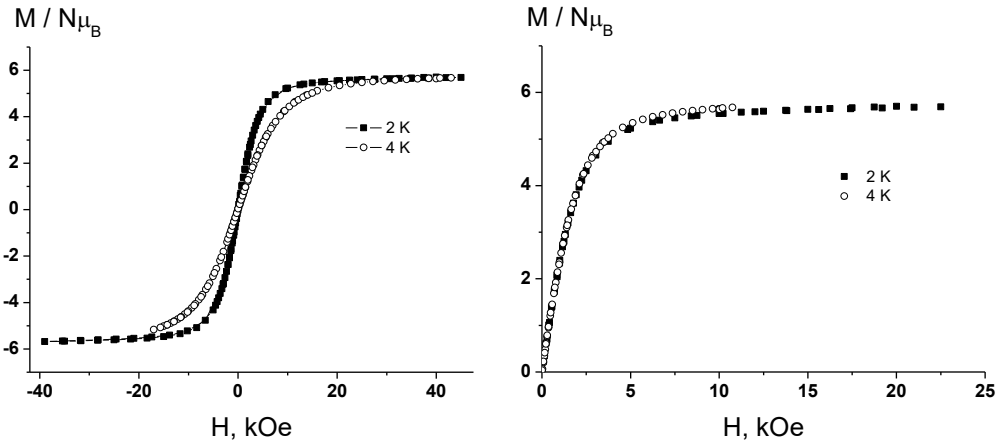

a *b*

Figure S38 Experimental dependencies of magnetization M vs H (*a*) and M vs (H/T) for complex **8**.

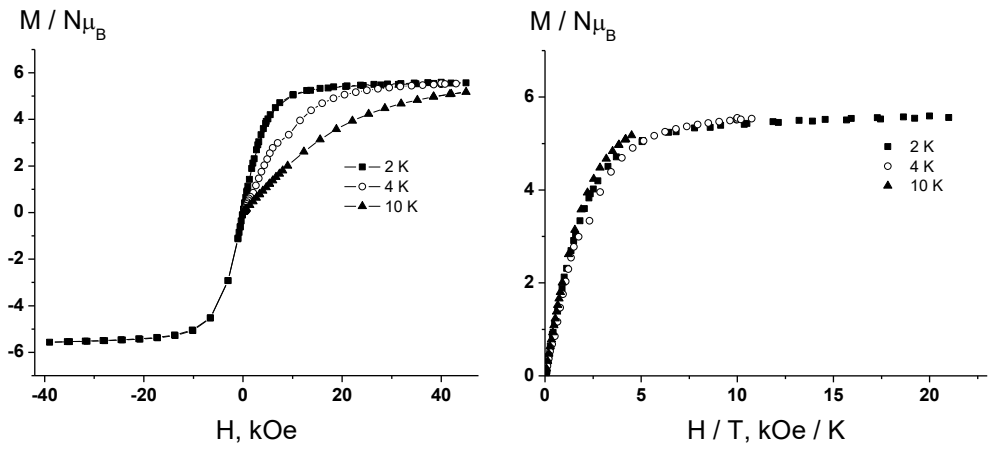

a *b*

Figure S39 Experimental dependencies of magnetization M vs H (*a*) and M vs (H/T) for complex **16**.